PLANT CELL

A gain-of-function allele of a DREB transcription factor gene ameliorates drought tolerance in wheat

Fangming Mei ,[1] Bin Chen ,[1] Linying Du ,[2] Shumin Li ,[1] Dehe Zhu ,[1] Nan Chen ,[1] Yifang Zhang ,[1] Fangfang Li ,[1] Zhongxue Wang ,[1] Xinxiu Cheng ,[1] Li Ding ,[1] Zhensheng Kang [1,3,4,*] and Hude Mao [1,3,*]

1   State Key Laboratory of Crop Stress Biology for Arid Areas, College of Plant Protection, Northwest A&F University, Yangling, Shaanxi 712100, China
2   State Key Laboratory of Crop Stress Biology for Arid Areas, College of Life Science, Northwest A&F University, Yangling, Shaanxi 712100, China
3   State Key Laboratory of Crop Stress Biology for Arid Areas, Pioneering Innovation Center for Wheat Stress Tolerance Improvement, Yangling, Shaanxi 712100, China
4   Yangling Seed Industry Innovation Center, Yangling, Shaanxi 712100, China

*Author for correspondence: kangzs@nwsuaf.edu.cn (Z.K.), mao_dehu@nwsuaf.edu.cn (H.M.)
These authors contributed equally (F.M. and B.C.).
H.M. and Z.K. conceived and supervised this study. F.M., L.D., S.L., D.Z., N.C., Y.Z., F.L., Z.W., X.C., L.D., and H.M. carried out experiments. B.C., H.M., and F.M. analyzed the data. H.M. and Z.K. wrote the manuscript with contributions from all the authors.
The authors responsible for the distribution of materials integral to the findings presented in this article in accordance with the policy described in the Instructions for Authors (https://academic.oup.com/plcell) is: Hude Mao (mao_dehu@nwsuaf.edu.cn).

Abstract

Drought is a major environmental factor limiting wheat production worldwide. However, the genetic components underlying wheat drought tolerance are largely unknown. Here, we identify a DREB transcription factor gene (*TaDTG6-B*) by genome-wide association study that is tightly associated with drought tolerance in wheat. Candidate gene association analysis revealed that a 26-bp deletion in the *TaDTG6-B* coding region induces a gain-of-function for TaDTG6-B^{Del574}, which exhibits stronger transcriptional activation, protein interactions, and binding activity to dehydration-responsive elements (DRE)/CRT cis-elements than the TaDTG6-B^{In574} encoded by the allele lacking the deletion, thus conferring greater drought tolerance in wheat seedlings harboring this variant. Knockdown of *TaDTG6-B*^{Del574} transcripts attenuated drought tolerance in transgenic wheat, whereas its overexpression resulted in enhanced drought tolerance without accompanying phenotypic abnormalities. Furthermore, the introgression of the *TaDTG6-B*^{Del574} elite allele into drought-sensitive cultivars improved their drought tolerance, thus providing a valuable genetic resource for wheat breeding. We also identified 268 putative target genes that are directly bound and transcriptionally regulated by TaDTG6-B^{Del574}. Further analysis showed that TaDTG6-B^{Del574} positively regulates *TaPIF1* transcription to enhance wheat drought tolerance. These results describe the genetic basis and accompanying mechanism driving phenotypic variation in wheat drought tolerance, and provide a novel genetic resource for crop breeding programs.

Introduction

Among the many effects of climate change that can severely disrupt agricultural production, water scarcity and the unpredictable nature of drought represent one of the largest threats to globally consumed staple crops, such as wheat

IN A NUTSHELL

Background: Wheat (*Triticum aestivum* L.) is produced in arid and semi-arid regions around the world, and water scarcity poses a constant threat to yields, with global climate change and population growth exacerbating this vulnerability. Thus, breeding drought-tolerant germplasm to improve yields in arid regions represents an important goal of wheat breeding programs. However, drought tolerance is a complex quantitative trait controlled by numerous genes that are involved in multiple drought-responsive signaling pathways and metabolic networks. Defining the genetic and molecular mechanisms responsible for drought tolerance is a necessary step toward accelerating breeding.

Question: What are the key regulatory genes responsible for variation in drought tolerance in wheat and how do they function in conferring a tolerant phenotype? This study aimed to identify genetic components contributing to variation in wheat drought tolerance and to develop molecular markers to facilitate development of elite drought-tolerant wheat varieties.

Findings: Through a genome-wide association study and candidate gene association analysis, we identified a 26-bp deletion in the *TaDTG6-B* coding region that induces a gain-of-function for the encoded TaDTG6-B^{Del574} protein, a transcription factor tightly associated with drought tolerance in wheat. TaDTG6-B^{Del574} exhibits stronger transcriptional activation, more protein interactions, and higher binding activity to DRE/CRT (dehydration-responsive element/C-repeat) cis-elements than the TaDTG6-B^{In574} that lacks the deletion. *TaDTG6-B*^{Del574} knockdown attenuated drought tolerance in transgenic wheat, whereas its overexpression led to significantly enhanced drought tolerance. No effect on drought tolerance was associated with changes in expression of *TaDTG6-B*^{In574} allele. TaDTG6-B^{Del574} positively regulated *TaPIF1* expression, thereby enhancing wheat drought tolerance. Furthermore, the introgression of the *TaDTG6-B*^{Del574} elite allele into drought-sensitive cultivars improved their drought tolerance, thus providing a valuable genetic resource for wheat breeding.

Next steps: Future and ongoing research will involve the determination of the crystal structure of TaDTG6-B variants and how they relate to drought tolerance in wheat. We also seek to dissect the regulatory networks between *TaDTG6-B*^{Del574} and other drought-responsive genes.

(*Triticum aestivum* L.), especially in arid and semi-arid regions. In particular, wheat production is often limited by insufficient water resources, with reduced irrigation leading to direct consequences on yield (Daryanto et al., 2016; Langridge and Reynolds, 2021). Due to this long-standing instability in the security of wheat production, breeding programs have increasingly focused their attention on improving elite, drought-tolerant cultivars that provide high yields with less water input or greater resilience to drought conditions. Regardless of advances in numerous agronomically valuable traits in wheat, drought sensitivity remains a prevalent fixture in widely cultivated commercial lines (Tester and Langridge, 2010; Lobell et al., 2014; Abberton et al., 2016; Bailey-Serres et al., 2019), which will be exacerbated by increasingly frequent severe drought events due to climate change (Lesk et al., 2016; Ault, 2020). This confluence of issues poses a threat to global food security, and thus highlights the urgency of resolving the complicated mechanisms of drought tolerance in wheat for agricultural research programs.

One leverage point to accelerate crop improvement is to better understand the genetic and molecular bases of drought tolerance. Over the past few decades, much research effort has been dedicated to investigating the molecular genetic and biochemical regulatory pathways and signal cascades that contribute to a drought-tolerant phenotype (Hu and Xiong, 2014; Zhu, 2016; Gong et al., 2020; Gupta et al., 2020; Zhang et al., 2021). However, decreased yield or biomass due to linkage drag or other physiological or developmental consequences in drought-tolerant plants is a persistent obstacle for the deployment of candidate markers in elite cultivars. Nevertheless, drought-tolerant alleles that have been lost through domestication or overlooked in local landraces represent a major genetic resource for breeders equipped with sufficiently sensitive tools to isolate their effects in high-throughput screens (Liang et al., 2021). For example, studies have refined the use of linkage disequilibrium (LD)-based genome-wide association study (GWAS) and candidate gene association analysis over the past two decades to identify several structural variants or alleles significantly related to drought response in plants (Liu et al., 2013, 2020; Mao et al., 2015, 2020; Wang et al., 2016; Xiang et al., 2017; Guo et al., 2018; Xiong et al., 2018; Blein-Nicolas et al., 2020; Li et al., 2020; Zhang et al., 2020; Wu et al., 2021). In our previous study, we performed GWAS and candidate gene association analysis to identify a 108-bp insertion present in the promoter of the NAC (NAM-ATAF-CUC2) transcription factor gene *TaNAC071-A*, which

contains two MYB cis-regulatory elements (CREs) and is strongly associated with drought tolerance between wheat accessions. These CREs can be directly bound by the wheat MYB transcription factor TaMYBL1 for the transcriptional activation of *TaNAC071-A*, subsequently conferring drought tolerance (Mao et al., 2022). However, exploring the contributing factors that determine drought tolerance remains difficult, largely due to the huge number of genes and the multiplicity of networks involved in balancing plant development and metabolic pathways under drought stress, in addition to complexities and redundancy inherent to the hexaploid wheat genome (IWGSC, 2018).

To respond to drought stress, the expression of a specific set of genes must be rapidly induced in response to external and internal cues of water deficit (Zhu, 2016; Gong et al., 2020; Zhang et al., 2021). In this process, dehydration-responsive element binding proteins/C-repeat binding factors (DREB/CBF) transcription factors (DREBs hereafter) are essential players in the transcriptional activation of the abscisic acid (ABA)-independent drought stress response via binding to dehydration-responsive elements (DREs, core motif: A/GCCGAC) in the promoters of drought-responsive genes (Yamaguchi-Shinozaki and Shinozaki, 2006; Nakashima et al., 2009; Agarwal et al., 2017). *DREBs* can be categorized as either *DREB1*-type or *DREB2*-type genes, and several studies have reported their function in adaptive responses to stress (Yamaguchi-Shinozaki and Shinozaki, 2006; Nakashima et al., 2009; Morran et al., 2011; Shavrukov et al., 2016; Agarwal et al., 2017; Yang et al., 2020; Zhou et al., 2020), suggesting their possible value as targets for reverse genetic improvement of drought tolerance in wheat. Therefore, a greater understanding of the genetic variation in *DREB* genes associated with drought tolerance in wheat will facilitate the development of superior, drought-adapted wheat varieties.

Here, we used GWAS to identify a case of allelic variation caused by a 26-bp insertion/deletion (InDel) polymorphism in the coding region of a DREB transcription factor gene, *TaDTG6-B*, that confers differential drought tolerance across wheat accessions. Molecular and transgenic analyses in wheat revealed that the 26-bp deletion (Del574) in the coding region of *TaDTG6-B* results in a gain-of-function for the TaDTG6-B^{Del574} protein, as it showed stronger transcriptional activation ability, protein–protein interactions, and binding to DRE/CRT cis-elements. These effects promoted drought stress-responsive gene expression, thereby enhancing drought tolerance over that of the TaDTG6-B^{In574} nonfunctional variant. We further show that TaDTG6-B^{Del574} binds to the promoter of *PHYTOCHROME-INTERACTING FACTOR1* (*TaPIF1*), upregulating its transcription and consequently inducing drought tolerance in wheat seedlings. Furthermore, the introgression of the 26-bp deletion allele into drought-sensitive cultivars improved their drought tolerance. These findings provide a major breakthrough in determining the genetic basis underlying phenotypic variation in wheat drought tolerance and reveal an important genetic target for breeding drought-tolerant wheat varieties.

Results

RNA-seq reveals abundant genetic diversity in wheat transcripts

To identify loci associated with drought tolerance in wheat, we conducted a GWAS using transcriptome deep sequencing (RNA-seq) to obtain a large set of informative single-nucleotide polymorphisms (SNPs) in wheat transcripts. We assembled a collection of 430 hexaploid wheat accessions from a previously characterized population that was used for the genetic dissection of several agronomic traits (Mao et al., 2020, 2022; Yu et al., 2020; Wu et al., 2021). We sequenced the transcriptomes of leaves at the three-leaf stage from all 430 accessions grown under well-watered conditions on an Illumina Hiseq platform, which generated ~10.35 Tb of 150-bp paired-end reads. After removing low-quality reads, we retained an average of 163.13 million reads per sample, resulting in ~70.15 billion high-quality reads. On average, 84.8% of the clean reads mapped to the wheat reference genome (IWGSC RefSeq v1.1), of which 92.15% mapped to annotated genes. Among the total reads that could be mapped to the genome, 90.4% matched a single gene; we therefore used these reads to build a consensus sequence for each sample (Supplemental Data Set 1). After quality control, we identified a total of 5,610,042 SNPs. Compared to the wheat reference genome, any given wheat accession carried an alternative allele at 230,579 loci on average, with a range of 105,167–355,776 SNPs.

We then used 1,921,782 SNPs with a missing data rate <0.6 for imputation to infer missing genotypes. Of these, we mapped 1,735,369 SNPs, accounting for 90.3% of the total SNPs, to genomic regions containing 65,263 high-confidence and 35,555 low-confidence genes. For the purpose of GWAS, we removed any SNP with a minor allele frequency (MAF) <5%, leaving 465,269 SNPs, which was substantially lower than the number of SNPs found for maize (*Zea mays*) (Fu et al., 2013; Liu et al., 2020) or lettuce (*Lactuca sativa*; Zhang et al., 2017) in similar diversity panels, suggesting the presence of fewer polymorphisms across wheat accessions. We also calculated the distribution of SNPs and genes along each chromosome using 1-Mb sliding windows (Figure 1; Supplemental Figure S1A). On all chromosomes, we observed that SNP density is low in regions surrounding the centromeres, which was in agreement with the low gene density of these genomic regions (Figure 1).

GWAS for wheat drought tolerance at the seedling stage

We merged the 465,269 SNPs above with 397,761 SNPs (missing rate <0.6 and MAF of at least 5%) from the wheat 660K SNP array (Supplemental Figure S1B) as representative genotypes of the GWAS panel. The merged data set consisted of 863,030 SNPs, which were relatively evenly distributed over each of the 21 wheat chromosomes (Supplemental Figure S1C). The genome-wide average inter-SNP distance was 16.86 kb and varied from 10.69 kb on chromosome 3B to 75.83 kb on 4D (Supplemental Data Set
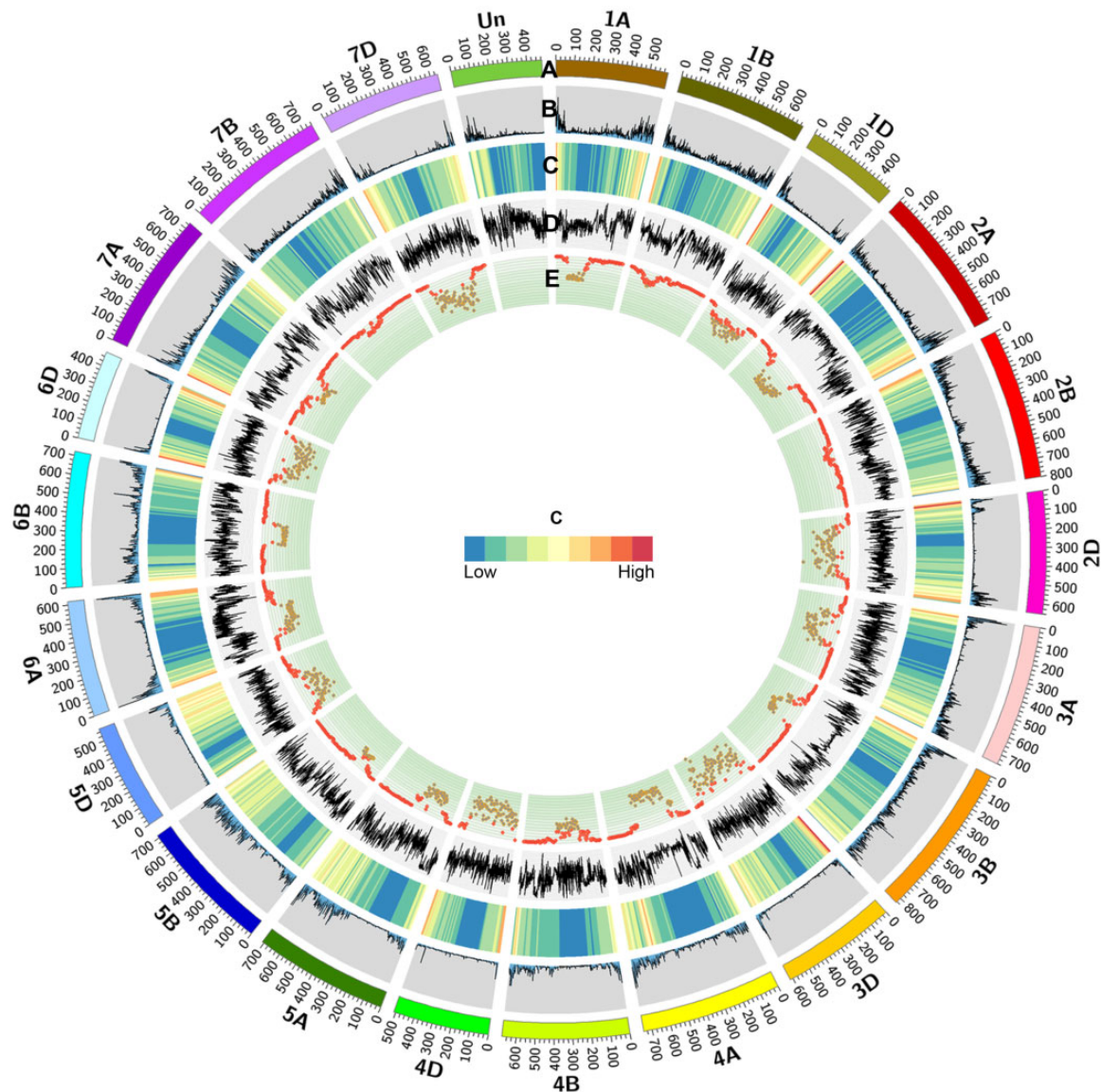
Figure 1 Circos diagram showing the global physical distribution of the 863,030 SNPs, average nucleotide diversity, and LD blocks for each chromosome. A, Physical size of each chromosome. Wheat chromosomes are represented in different colors. B, SNP distribution is represented by SNP numbers in 1-Mb windows for each chromosome. C, Heatmap representation of the number of matched high-confidence genes in 1-Mb windows for each chromosome. D, Average nucleotide diversity, as estimated by polymorphism contents using a 1-Mb sliding window along the chromosomes. E, LD block sizes for SNPs within a 5-Mb sliding window.

2). Based on the IWGSC (International Wheat Genome Sequencing Consortium) wheat reference genome annotation (v1.1), the 863,030 SNPs were mainly located in coding sequences (40%), of which 44.45% (or 17.8% of all SNPs) caused nonsynonymous mutations. The remaining SNPs were located in intergenic regions (20.1%), introns (15.0%), 5′-untranslated regions (5′-UTRs, 2.5%), and 3′-UTRs (6.3%) (Supplemental Figure S1D). We clustered the 430 wheat accessions with this SNP dataset into six subpopulations based on population structure, kinship, and principle component analyses. We also calculated the LD decay distance to be 5.02 Mb for the full set of SNP markers with an r^2 cut-off value set to 0.1 (Supplemental Figure S2), and estimated the significant threshold P-value at 1.38×10^{-5} for

marker–trait associations (MTAs; Supplemental Data Set 2). The average genome-wide LD block size was 2.49 Mb, with averages of 2.19 Mb, 1.92 Mb, and 4.25 Mb for the A, B, and D subgenomes, respectively (Figure 1E; Supplemental Data Set 3).

Drought tolerance is a complex quantitative trait that is affected by both the timing and the severity of the stress imposed on plant growth and development (Wang et al., 2016; Tardieu et al. 2018). Survival rate (SR) index after severe drought stress has been widely used for identifying drought-tolerant genes due to its reliability as an indicator of water conservation in drought-stressed plants (Wang et al., 2016; Xiang et al., 2017; Liu et al., 2020; Mao et al., 2020). We therefore used SR to rate the tolerance of wheat
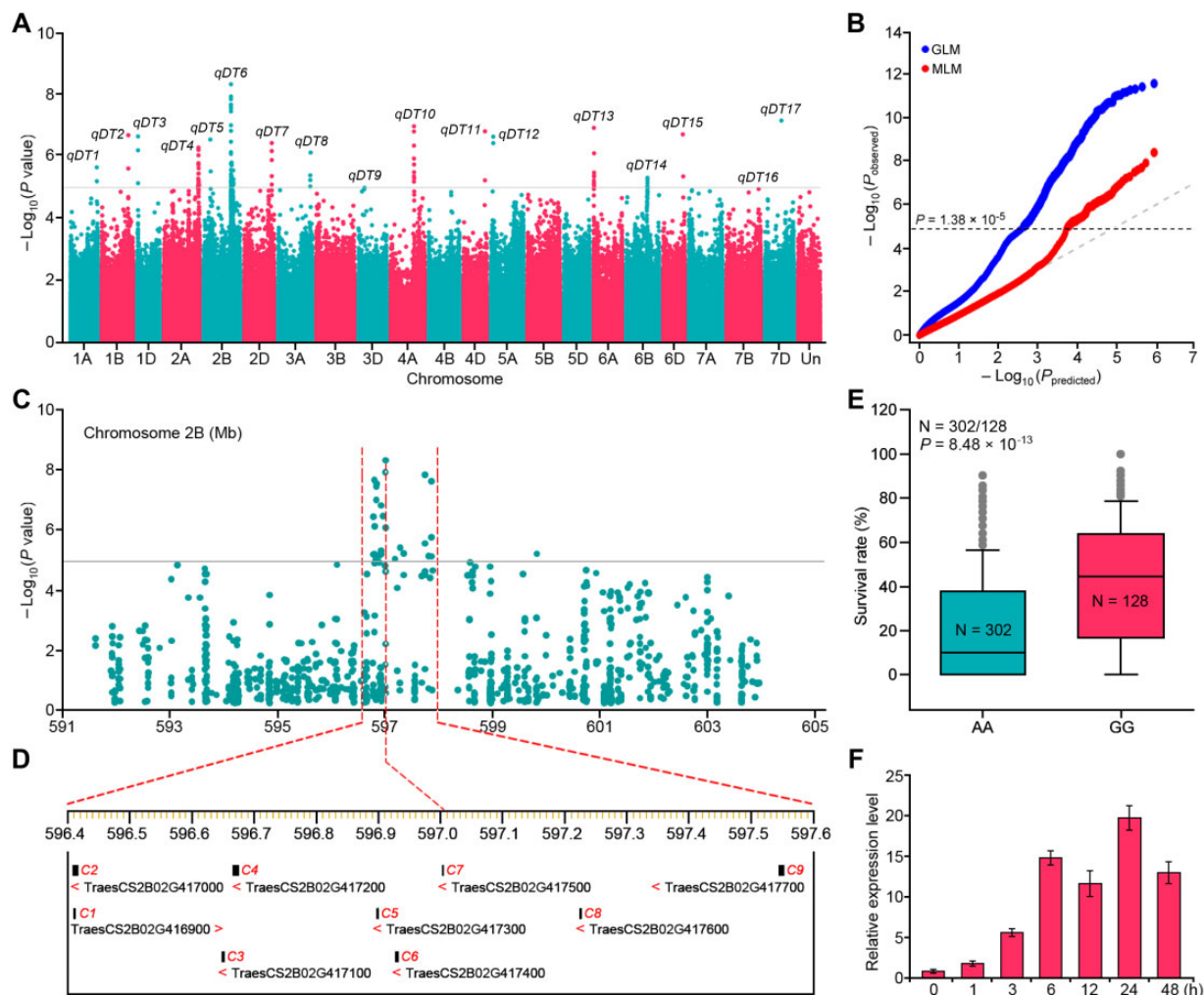
Figure 2 *TaDTG6-B* confers natural variation in drought tolerance of wheat seedlings. A, Results of GWAS for wheat drought tolerance. The gray horizontal line indicates the genome-wide significance threshold ($P = 1.38 \times 10^{-5}$). B, Quantile-quantile plot for GWAS results under a general linear model (GLM) and MLM. C, Genome-wide association signals for wheat drought tolerance, shown over the 591–605 Mb region of chromosome 2B. D, Filtered gene models within the candidate region on chromosome 2B. E, SR for the two genotypes at the leading SNP on chromosome 2B. Statistical significance was determined by analysis of variance (ANOVA) ($n = 302$ for genotype A; $n = 128$ for genotype G). F, Relative expression levels of *TaDTG6-B* under drought stress. Values are means ± sd ($n = 3$).

seedlings to severe drought stress because of the relatively high reproducibility of this phenotype under these conditions. To this end, we scored each accession for SR under severe water limitation, which revealed a high degree of variation among wheat accessions in repeated phenotypic assays, ranging from 0% to 96.8% (Supplemental Data Set 4). To identify the loci underlying this phenotype, we conducted a GWAS based on the best linear unbiased prediction of SR index using the 863,030 SNPs (Mao et al., 2022). Under the standard mixed linear model (MLM), we obtained 109 SNPs significantly associated with drought tolerance ($P < 1.38 \times 10^{-5}$; Figure 2, A and B; Supplemental Data Set 5). The 109 MTAs formed 17 genomic regions based on LD blocks, with 284 candidate genes located within these intervals. Of these, 78 were upregulated and 61

genes were downregulated upon drought stress (Supplemental Data Set 6). Gene ontology (GO) analysis showed that the 284 candidate genes are linked to biological pathways involved in plant stress response (Supplemental Figure S3), including several genes related to drought stress, such as wheat homologs of Arabidopsis *TREHALOSE-6-PHOSPHATE SYNTHASE1* (*TPS1*; Gómez et al., 2010), *VASCULAR PLANT ONE ZINC FINGER PROTEIN1* (*VOZ1*; Nakai et al., 2013), *DREB1A* (Kasuga et al., 1999), *ANAC2* (Wu et al., 2009), *ALDEHYDE DEHYDROGENASE 3H1* (*ALDH3H1*; Kirch et al., 2001), *NAC WITH TRANSMEMBRANE MOTIF 1-LIKE 4* (*NTL4*; Lee et al., 2012), *TIP GROWTH DEFECTIVE1* (*TIP1*; Hemsley et al., 2005), and *ARABIDOPSIS VACUOLAR H$^+$-PYROPHOSPHATASE1 AVP1* (Gaxiola et al., 2001; Supplemental Data Set 6). The other

genes were predicted to be involved in transport, development, and metabolism, among other processes (Supplemental Figure S3).

TaDTG6-B is significantly associated with drought tolerance

At a local scale, we observed a significant association between wheat drought tolerance and 29 SNPs and 9 candidate genes within one LD block located in the 596.4–597.6 Mb (*qDT6*) genomic region on chromosome 2B (Figure 2, C and D). The leading SNP, Chr2B_597008433, was located 5,524-bp upstream of the translation start codon for a *DREB* gene, TraesCS2B02G417500, at which position an adenine (A) and a guanine (G) were associated with lower and greater drought tolerance, respectively (Figure 2E). In addition, TraesCS2B02G417500 was expressed at higher levels in seedling leaves (Supplemental Figure S4A) and was the most strongly upregulated (over 27-fold) among the nine candidate genes under drought stress conditions (Supplemental Data Set 6). We confirmed this result by reverse transcription–quantitative polymerase chain reaction (RT–qPCR) analysis (Figure 2F; Supplemental Figure S4B). Since previous studies have shown that *DREB* genes can perform major roles in plant responses to abiotic stress (Yamaguchi-Shinozaki and Shinozaki, 2006; Nakashima et al., 2009; Agarwal et al., 2017), we hypothesized that TraesCS2B02G417500 is a likely candidate for the *qDT6* locus, which we designated *TaDTG6-B*.

In light of the significant association between *TaDTG6-B* and drought tolerance in wheat seedlings, we aimed to validate its MTS by sequencing the ~3.2-kb *TaDTG6-B* locus in 281 wheat accessions. We thus identified 14 SNPs and 3 InDels. MLM-based candidate gene association analysis revealed that two significant SNPs/InDels ($P < 1.38 \times 10^{-5}$; InDel574 and SNP644) are located within the *TaDTG6-B* coding region. The 26-bp InDel (InDel574) was located 574-bp downstream of the predicted start codon and showed the most significant association with SR ($P = 4.68 \times 10^{-8}$; Figure 3A; Supplemental Data Set 7). We estimated the pairwise LD of these SNP and InDel markers, which indicated that InDel574 is in strong LD with SNP614 and SNP644 ($r^2 \geqslant 0.6$), but in low LD with other variants (Figure 3B). Moreover, we also determined that wheat accessions carrying the *TaDTG6-B*^{Del574} allele lacking the 26-bp insertion have significantly higher SR than those harboring the *TaDTG6-B*^{In574} allele ($P = 1.04 \times 10^{-13}$; Figure 3C), leading us to designate the *TaDTG6-B*^{Del574} allele as the drought-tolerant allele. In addition, *TaDTG6-B* expression levels did not significantly differ between wheat accessions when separated based on the InDel574 allele they carry (Figure 3D).

Next, we compared the effects of the *TaDTG6-B*^{Del574} and *TaDTG6-B*^{In574} alleles on drought tolerance in wheat by introducing the *TaDTG6-B*^{Del574} allele from the drought-tolerant wheat cultivar Jinmai47 into two drought-sensitive wheat cultivars carrying the *TaDTG6-B*^{In574} allele (Yangmai13 and GLUYAS EARLY) to generate near-isogenic

lines (NILs; Supplemental Figure S5A). We then subjected the two BC$_4$F$_2$ populations to drought stress and genotyping for InDel574 (Figure 3, E and F). We observed that the *TaDTG6-B*^{Del574} allele co-segregates with drought tolerance in these two populations (Supplemental Figure S5, B and C). Furthermore, we subjected the progeny homozygous for each allele (NIL-*TaDTG6-B*^{Del574} and NIL-*TaDTG6-B*^{In574}) to drought conditions, and calculated the resulting plant SRs after stress and re-watering to quantify the phenotypic contribution of each *TaDTG6-B* allele to drought tolerance. We determined that the average SR of NIL-*TaDTG6-B*^{Del574} homozygous plants is higher than that seen with NIL-*TaDTG6-B*^{In574} plants (Figure 3G), supporting the premise that the *TaDTG6-B*^{Del574} allele could enhance drought tolerance. Based on these collective results, we suggest that the 26-bp InDel is the likely cause of phenotypic differences in drought tolerance associated with *TaDTG6-B*, and therefore the *TaDTG6-B*^{In574} is the drought-sensitive allele, while *TaDTG6-B*^{Del574} is the drought-tolerant allele.

The *TaDTG6-B*^{Del574} and *TaDTG6-B*^{In574} alleles encode DREB TFs with different function

TaDTG6-B encodes a DREB TF, belonging to a family with more than 110 members in the wheat genome (Supplemental Figure S6). The canonical DREB proteins belong to the A-1 (DREB1) and A-2 (DREB2) subgroups (Nakashima et al., 2009; Liu et al., 2013). Notably, the number of DREB1 subfamily members ($n = 89$) in wheat was approximately 15-fold greater than in Arabidopsis (with six members), and 9-fold that in rice (*Oryza sativa*; 10 members) or maize (10) DREB1s, indicating that the DREB1 family is greatly expanded in wheat. Phylogenetic analysis showed that TaDTG6-B is an ortholog of OsDREB1E in rice and ZmDREB1.10 in maize (Supplemental Figure S6). In addition, since hexaploid wheat possesses three subgenomes ($2n = 6x = 42$; AABBDD), we looked for the homoeologs in the other two subgenomes, *TaDTG6-A* (TraesCS2A02G399500) and *TaDTG6-D* (TraesCS2D02G397000). Comparison of the *TaDTG6-A*, *TaDTG6-D*, *TaDTG6-B*^{Del574}, and *TaDTG6-B*^{In574} coding regions indicated that only the homoeolog from subgenome B harbors the 26-bp deletion, which results in a frameshift mutation that introduces a premature stop codon (Supplemental Figure S7). Due to this stop codon, the predicted protein sequence of TaDTG6-B is four amino acids shorter than that of its homoeologs and carries missense mutations leading to an altered peptide sequence over the 21 C-terminal residues (Figure 4A). We thus speculated that this genetic variation in *TaDTG6-B* may potentially cause differences in protein activity between the TaDTG6-B^{Del574} and TaDTG6-B^{In574} variants.

To test this hypothesis, we conducted transient expression assays using a ~2.0-kb promoter fragment from *TaDTG6-A*, *TaDTG6-D*, *TaDTG6-B*^{Del574}, and *TaDTG6-B*^{In574} to evaluate their respective ability to drive the transcription of the firefly luciferase reporter gene (*LUC*) in wheat protoplasts. We determined that the *TaDTG6-B*^{Del574}*pro*:*LUC* and *TaDTG6-*
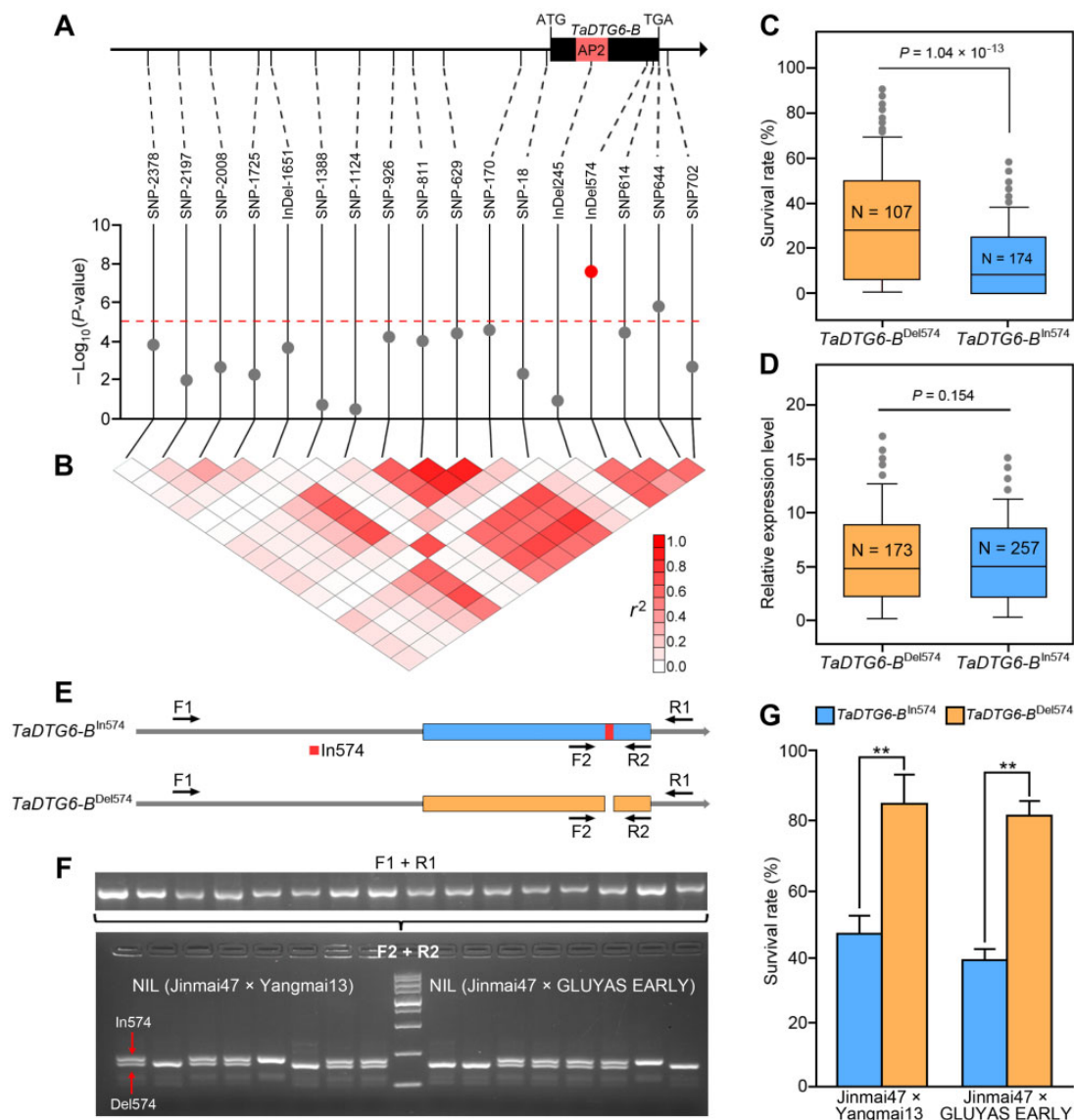
Figure 3 The *TaDTG6-B*^{Del574} allele is associated with drought tolerance in wheat seedlings. A, Association analysis between genetic variation at *TaDTG6-B* and drought tolerance. A schematic diagram of the ~3.2-kb *TaDTG6-B* genomic region is shown at the top. The region encoding the AP2 domain is indicated in red. B, Pattern of pairwise LD for each polymorphism over the *TaDTG6-B* locus. C, Distribution of the SR for the two genotype groups based on InDel574 (Del574 and In574). D, Relative expression levels of *TaDTG6-B* in the two genotype groups based on InDel574. Statistical significance was determined by ANOVA. E, Schematic diagram of the primers used for two-round PCR genotyping of InDel574. F, Molecular marker (InDel574) selection of segregating NILs homozygous for either the *TaDTG6-B*^{Del574} or *TaDTG6-B*^{In574} alleles. G, Drought tolerance of the NILs carrying the tolerant allele *TaDTG6-B*^{Del574} or the sensitive allele *TaDTG6-B*^{In574}. Values are means ± SD from three independent experiments; statistical significance was determined by two-sided Student's t test (**$P < 0.01$).

B^{In574}*pro:LUC* reporter constructs are characterized by relatively higher transcription levels than that of *TaDTG6-Apro:LUC* and *TaDTG6-Dpro:LUC*. However, we detected no significant differences in the luciferase activity derived from the *TaDTG6-B*^{Del574}*pro:LUC* and *TaDTG6-B*^{In574}*pro:LUC* reporters (Figure 4B), indicating that any sequence variation in the *TaDTG6-B* promoter region does not affect promoter activity. We also conducted fluorescence microscopy to assess the subcellular localization of each isoform by independently transfecting wheat protoplasts with the constructs *35S:TaDTG6-A-GFP*, *35S:TaDTG6-D-GFP*, *35S:TaDTG6-B*^{Del574}-*GFP*, *35S:TaDTG6-B*^{In574}-*GFP*, and the empty vector control *GFP* (encoding green fluorescent protein). We clearly detected green fluorescence for all four *TaDTG6* constructs in the nucleus, while the GFP signal of the control plasmid was evenly distributed in both the cytoplasm and the nucleus (Figure 4C). These results suggested that TaDTG6-A, TaDTG6-D, TaDTG6-B^{Del574}, and TaDTG6-B^{In574} all localize to the nucleus and may therefore function as transcriptional regulators.

To further determine the differences in protein activity, we performed yeast transactivation assays using the full-
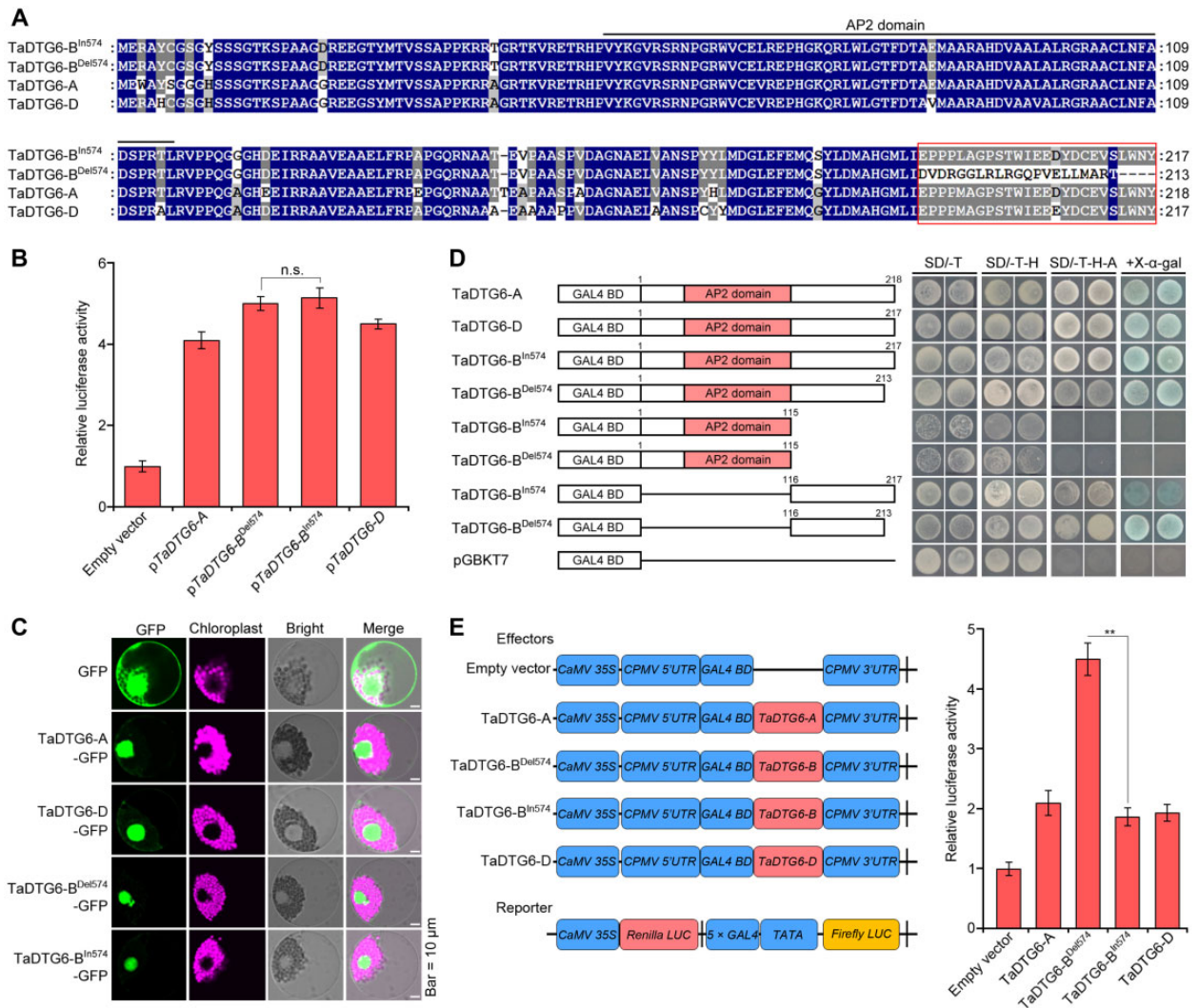
Figure 4 Molecular characterization of the TaDTG6-B^Del574 and TaDTG6-B^In574 variants. A, Amino acid sequence alignment of TaDTG6-A, TaDTG6-B^Del574, TDTG6-B^In574, and TaDTG6-D. The core AP2 domain is indicated with a black line and the 26-bp InDel inducing a frameshift is highlighted in the red box. B, Transient expression assays of the *TaDTG6-A*, *TaDTG6-B^Del574*, *TaDTG6-B^In574*, and *TaDTG6-D* promoters driving the transcription of the firefly *LUC* reporter gene in *N. benthamiana* leaves. C, Subcellular localization of GFP-tagged TaDTG6-A, TaDTG6-B^Del574, TaDTG6-B^In574, and TaDTG6-D in wheat protoplasts transfected with the respective encoding constructs. Scale bars, 10 μm. D, Evaluation of transactivation activity of TaDTG6-A, TaDTG6-B^Del574, TaDTG6-B^In574, and TaDTG6-D fused to the DNA-binding domain of yeast GAL4 via one-hybrid transactivation assays. The predicted conserved AP2 domain is shown in red in the schematic diagrams of the constructs (left). Yeast growth is shown (right) on SD medium lacking Trp (SD −T), Trp and His (SD −T–H), Trp, His, and Ade (SD −T, −H, −A), and SD −T, −H, −A + X-α-gal. E, Analysis of transcriptional activation by TaDTG6-A, TaDTG6-B^Del574, TaDTG6-B^In574, and TaDTG6-D in *N. benthamiana* leaves. Left shows the schematic diagrams of the effector constructs; right shows relative LUC activity. Values represent means ± SD from at least three independent experiments. Statistical significance was determined by two-sided Student's *t* test (**$P < 0.01$).

length coding sequence of *TaDTG6-A*, *TaDTG6-D*, *TaDTG6-B^Del574*, and *TaDTG6-B^In574*, and a set of *TaDTG6-B^Del574* and *TaDTG6-B^In574* truncated versions (Figure 4D, left). We observed that TaDTG6-A, TaDTG6-D, and both the TaDTG6-B^Del574 and TaDTG6-B^In574 exhibit transactivation activity, but transactivation was abolished in variants lacking the C terminus after the APETALA2 (AP2) domain (Figure 4D, right). These results indicated that the region necessary for transactivation is located in the C terminus of both TaDTG6-B variants. In addition, dual-luciferase reporter assays showed that a fusion between the yeast GAL4 DNA-binding domain and TaDTG6-A, TaDTG6-D, TaDTG6-B^Del574, or TaDTG6-B^In574 all enhance the transcription of a *LUC* reporter driven by a cauliflower mosaic virus (CaMV) 35S minimal promoter with GAL4 upstream activating sequences, suggesting that all proteins can induce transcriptional activity in planta. Notably, TaDTG6-B^Del574 exhibited stronger activity for transcriptional activation than TaDTG6-B^In574 (Figure 4E).

To further examine differences between the binding affinities of TaDTG6-B^Del574 and TaDTG6-B^In574 for their cofactors, we performed a yeast two-hybrid (Y2H) screen using the full-
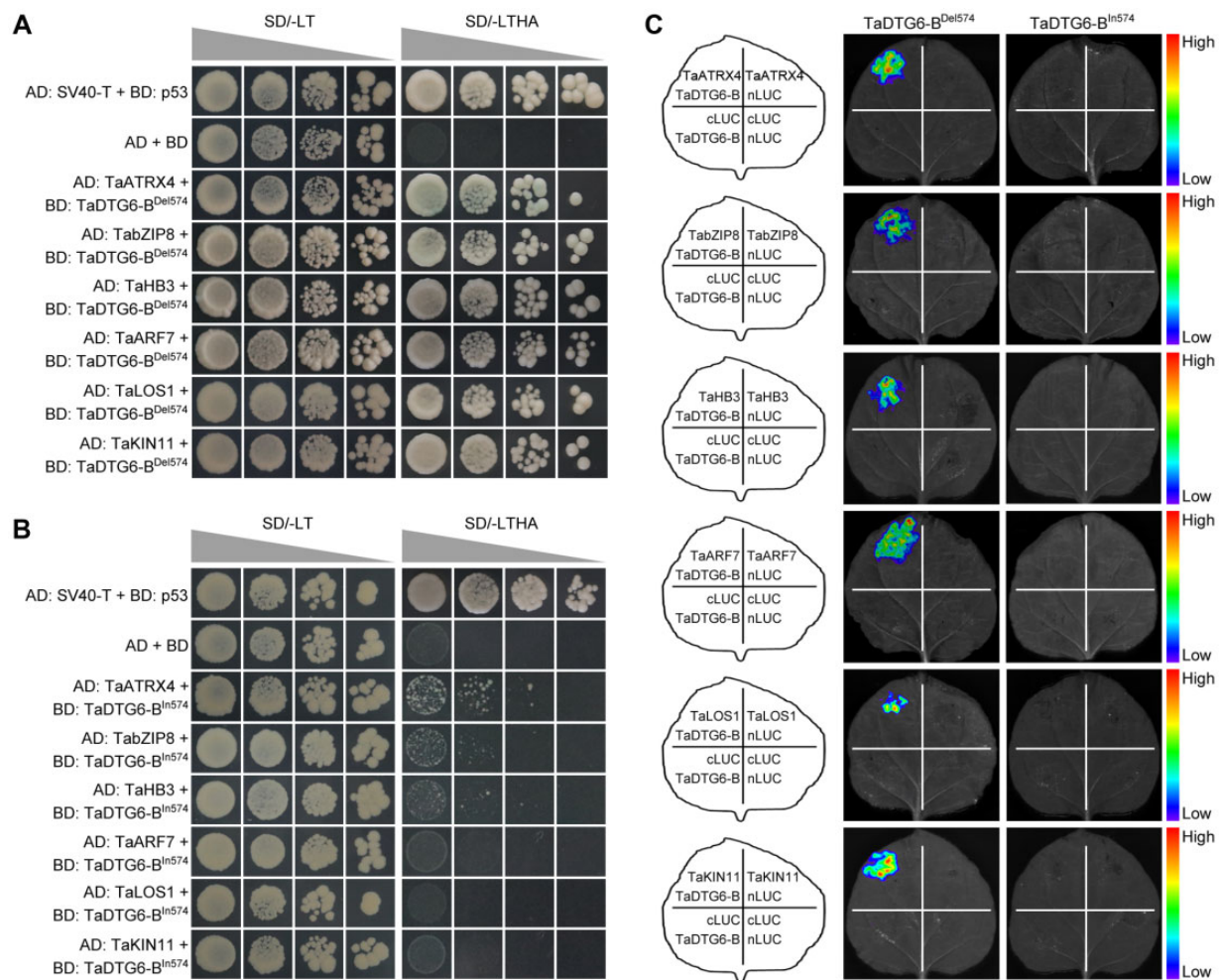
Figure 5 Screens for TaDTG6-B[Del574] and TaDTG6-B[In574] interaction with their cofactors. A, Y2H assays confirming the interactions between TaDTG6-B[Del574] and six cofactors. B, Y2H assays testing for interaction between TaDTG6-B[In574] and six cofactors of TaDTG6-B[Del574]. Yeast cells were grown on SD medium −Ade −His −Leu −Trp. AD, GAL4 activation domain; BD, GAL4 DNA-binding domain. C, Firefly LCI assays to further assess TaDTG6-B[Del574] and TaDTG6-B[In574] interactions with six cofactors in *N. benthamiana* leaves.

length coding sequences of *TaDTG6-B[Del574]* and *TaDTG6-B[In574]* cloned in-frame into pGBKT7 as baits. After two replicates of the screen, we identified 67 potential interacting proteins for TaDTG6-B[Del574] (Supplemental Data Set 8), but only nine potential interactors for TaDTG6-B[In574] (Supplemental Data Set 9). The set of potential TaDTG6-B[Del574] interactors included several proteins related to multicellular organism development, nucleotide and protein metabolism, protein modification, and stress response (Supplemental Figure S8), such as TaATRX4 (Alpha Thalassemia-mental Retardation X-linked4, also named SDG38 [SET DOMAIN PROTEIN 38]), TabZIP8 (Basic leucine-zipper 8), TaARF7 (Auxin response factor 7), TaHB3 (HOMEOBOX 3), TaLOS1 (LOW EXPRESSION OF OSMOTICALLY RESPONSIVE GENES1), and TaKIN11 (SNF1 KINASE HOMOLOG 11). We confirmed these interactions by targeted Y2H and luciferase complementation imaging (LCI) assays (Figure 5, A and C). However, we detected no interactions between TaDTG6-B[In574] and any of the TaDTG6-B[Del574] interactors (Figure 5, B and C), suggesting that the 26-bp insertion in the coding sequence of *TaDTG6-B* greatly reduces TaDTG6-

B[In574]-binding specificity to different interacting partners. Collectively, these results indicated that TaDTG6-B[Del574] has a higher capacity for transcriptional activation and protein interactions than TaDTG6-B[In574].

TaDTG6-B has a function in wheat drought tolerance

To dissect the function of TaDTG6-B[Del574] and TaDTG6-B[In574] in regulating plant drought tolerance, we generated transgenic lines overexpressing either *TaDTG6-B[Del574]* (*35S:TaDTG6-B[Del574]*) or *TaDTG6-B[In574]* (*35S:TaDTG6-B[In574]*) lines in Arabidopsis. We then selected three independent lines for each construct with high relative *TaDTG6-B* transcript levels for analysis (Supplemental Figure S9A). Three-week-old plants growing under favorable water conditions were exposed to drought stress for ∼20 days. After inducing drought stress followed by a 6-day recovery period with full irrigation, we saw that *35S:TaDTG6-B[Del574]* transgenic lines display higher drought tolerance than *35S:TaDTG6-B[In574]* transgenic and wild-type (WT) plants. However, the drought tolerance of

35S:TaDTG6-B[In574] transgenic and WT plants did not differ (Supplemental Figure S9, B and C).

To determine if the *TaDTG6-B*[Del574] allele was directly associated with elevated drought tolerance in wheat, we next generated *Ubipro:TaDTG6-B*[Del574] and *Ubipro:TaDTG6-B*[In574] T₃ transgenic overexpression (OE) lines using the full-length coding sequences of *TaDTG6-B*[Del574] and *TaDTG6-B*[In574] driven by the *Ubiquitin* promoter in the wheat cultivar Fielder, which carries the *TaDTG6-B*[Del574] allele and also harbors the *TaDTG6-A* and *TaDTG6-B* homoeologs with the same insertion as the *TaDTG6-B*[In574] allele. Immunoblot (IB) and RT–qPCR assays confirmed that *TaDTG6-B* transcription and TaDTG6-B protein abundance are both significantly higher in the transgenic *Ubipro:TaDTG6-B*[Del574] and *Ubipro:TaDTG6-B*[In574] OE lines relative to the nontransgenic parent (Figure 6, A and D). Soil-grown three-leaf stage seedlings under favorable water conditions were exposed to drought stress for ~25 days. After re-watering for 3 days, all *TaDTG6-B*[In574] transgenic OE lines exhibited drought tolerance comparable to that of WT plants (Figure 6, B and C). However, the drought tolerance of *Ubipro:TaDTG6-B*[Del574] OE lines was significantly higher than that of the WT (Figure 6, E and F). To confirm these effects, we knocked down *TaDTG6-B*[Del574] transcript levels using RNA interference (RNAi) in three independent lines of the wheat cultivar Fielder; all RNAi lines exhibited lower *TaDTG6-B* transcript and TaDTG6-B protein levels (Figure 6G), as well as lower drought tolerance than the WT (Figure 6, H and I). Notably, we observed no obvious abnormalities or morphological differences between the *Ubipro:TaDTG6-B*[Del574] transgenic and WT plants at either the seedling or adult plant stages under well-watered growth conditions (Figure 6, F and I; Supplemental Figure S10). These results clearly indicated that TaDTG6-B[Del574] function could serve as a determinant in plant drought tolerance, and further demonstrated that *TaDTG6-B*[Del574] is an elite allele for the improvement of wheat drought tolerance.

In addition, prior research had shown that breeding programs can progressively accumulate favored alleles (Barrero et al., 2011). Our genotyping analysis revealed that none of the 47 tetraploid wheat accessions tested here have the *TaDTG6-B*[Del574] elite allele. However, 44% (or 66 accessions) of a set of 150 hexaploid wheat landraces (Supplemental Data Set 10) carry *TaDTG6-B*[Del574], while only 33% (or 99 accessions) from a set of 300 modern cultivars (Supplemental Data Set 11) harbored this allele (Figure 6J), suggesting that the *TaDTG6-B*[Del574] allele might have occurred after the formation of hexaploid wheat and this elite allele has not been widely utilized in modern wheat breeding programs. Collectively, these results suggest that the *TaDTG6-B*[Del574] allele could be a promising resource for breeding to improve drought tolerance in wheat.

TaDTG6-B[Del574] binds to DRE/CRT cis-elements to regulate the expression of stress-responsive genes

To characterize the regulatory network required for TaDTG6-B[Del574] function in wheat drought tolerance, we compared the transcriptomes of the *Ubipro:TaDTG6-B*[Del574] OE wheat lines with those of WT plants under well-watered and water-deficit conditions. This RNA-seq analysis revealed 2,307 differentially expressed genes (DEGs, fold-change [FC] > 2 or FC < 0.5, $P < 0.01$) in the *TaDTG6-B*[Del574] OE lines relative to WT under well-watered conditions, consisting of 1,394 upregulated and 913 downregulated DEGs (Supplemental Figure S11 and Supplemental Data Set 12). In contrast, we identified 1,779 DEGs (FC > 2 or FC < 0.5, $P < 0.01$) in the OE lines relative to WT under water-deficit conditions, with 1,167 upregulated and 612 downregulated DEGs (Supplemental Figure S12 and Supplemental Data Set 13). GO analysis suggested that the combined upregulated genes from well-watered and water-deficit conditions are significantly enriched for terms related to stress responses, such as "response to water deprivation", "response to abscisic acid", "response to cold", "response to osmotic stress", and "cold acclimation"; the downregulated genes were significantly enriched for terms related to "photosynthesis", "flavonoid catabolic process", "oxidation–reduction process", and "response to cytokinin" (Supplemental Figure S11 and Supplemental Figure S12). These results suggest that TaDTG6-B[Del574] may be involved in multiple, overlapping regulatory networks responsible for inducing a higher tolerance in wheat response to drought stress.

To identify the DNA-binding sites and target genes of TaDTG6-B[Del574] and to better understand the possible mechanism(s) by which TaDTG6-B[Del574] improves wheat drought tolerance, we performed DNA affinity purification sequencing (DAP-seq; (O'Malley et al., 2016; Bartlett et al., 2017). Based on DAP-seq data obtained from two biological replicates, we identified 1,206 binding sites for TaDTG6-B[Del574] that mapped to 976 loci. These binding sites were located within genes or their flanking regulatory sequences, such as 2 kb of upstream sequences presumed to correspond to the promoter regions and 2 kb of downstream sequences predicted to contain the terminator regions. Further analysis revealed that 81.1%, 10.2%, and 8.7% of the TaDTG6-B[Del574] binding sites are present in defined promoter regions, gene bodies, and terminator regions, respectively (Figure 7A). By combining the results of DAP-seq and RNA-seq analyses, we predicted 268 genes as being putative direct binding targets for transcriptional regulation by TaDTG6-B[Del574]. Among these candidates, 154 genes were upregulated and 114 genes were downregulated in *TaDTG6-B*[Del574] OE plants (Figure 7B; Supplemental Data Set 14). GO analysis of these TaDTG6-B[Del574] target genes indicated that they are enriched in terms related to stress response, such as "response to water deprivation", "response to abscisic acid", "response to cold", and "response to osmotic stress" (Figure 7C), indicating that TaDTG6-B[Del574] initiates patterns of stress-responsive gene expression that facilitate an adaptive response to drought stress.

We then turned to MEME-ChIP (Machanick and Bailey, 2011) to predict potential TaDTG6-B[Del574] binding motifs based on the consensus sequences of the detected binding
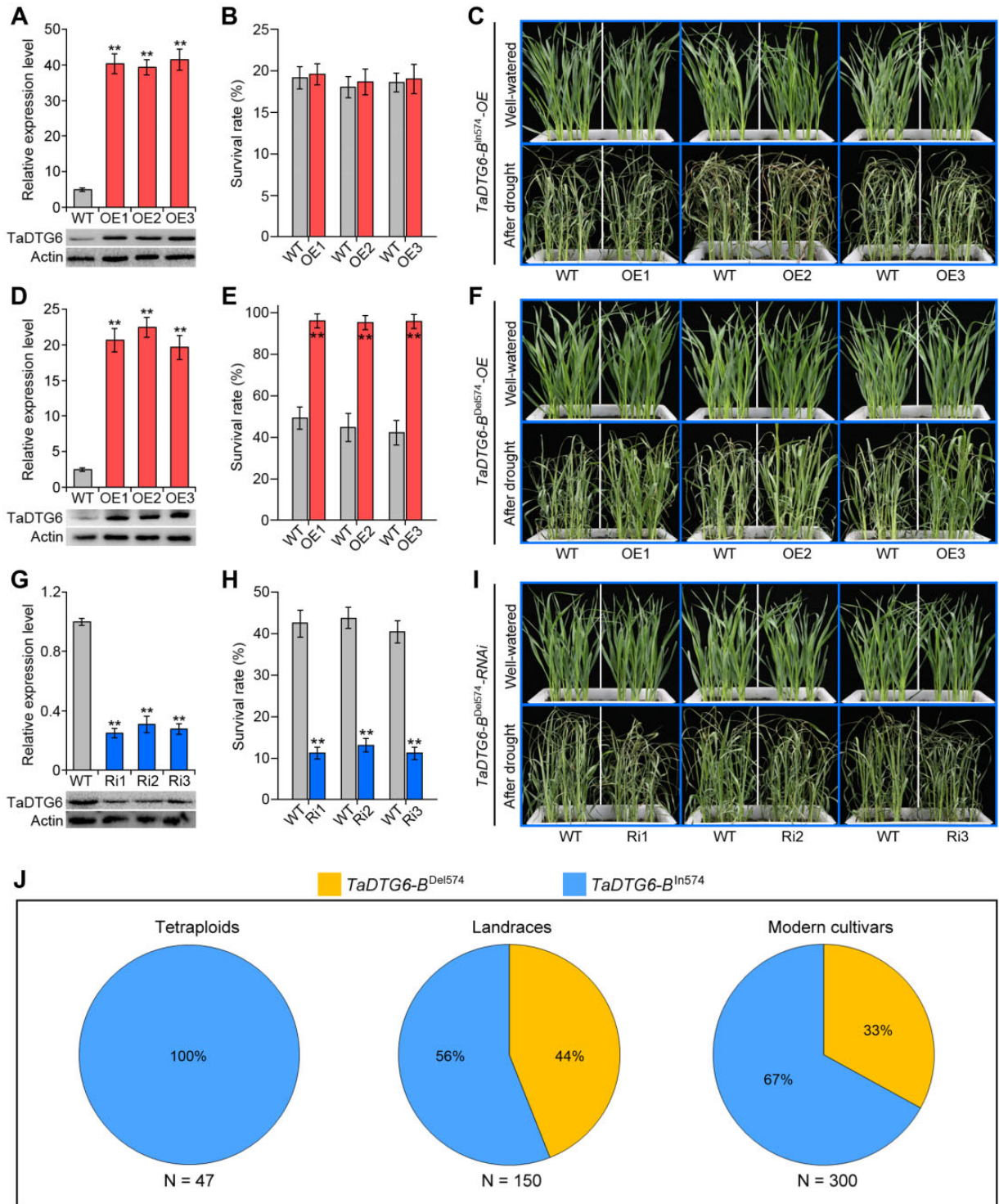
Figure 6 TaDTG6-B^{Del574} improves wheat drought tolerance. A, D, G, Relative expression levels of *TaDTG6-B* in *Ubipro:TaDTG6-B*^{In574} OE lines (A), *Ubipro:TaDTG6-B*^{Del574} OE lines (D), and *TaDTG6-B* RNAi (Ri) lines (G), as determined by RT–qPCR. Immunoblot of TaDTG6-B in WT and transgenic lines are shown below the RT–qPCR results. B, E, H, SRs in *Ubipro:TaDTG6-B*^{In574} OE lines (B), *Ubipro:TaDTG6-B*^{Del574} OE lines (E), and *TaDTG6-B* RNAi lines (H) during drought treatment and recovery. Seedlings with green and expanded viable leaves were regarded as survivors. Values are means ± SD from at least three independent experiments; statistical significance was determined by a two-sided Student's *t* test (**$P <$ 0.01). C, F, and I, Representative drought tolerance phenotypes in *Ubipro:TaDTG6-B*^{In574} OE lines (C), *Ubipro:TaDTG6-B*^{Del574} OE lines (F), and *TaDTG6-B* RNAi lines (I). Photographs were taken under well-watered conditions before drought treatment and after a 3-day period of recovery with full irrigation post drought treatment. J, Distribution of *TaDTG6-B*^{In574} and *TaDTG6-B*^{Del574} alleles in tetraploid wheat, hexaploid landraces, and modern cultivars.
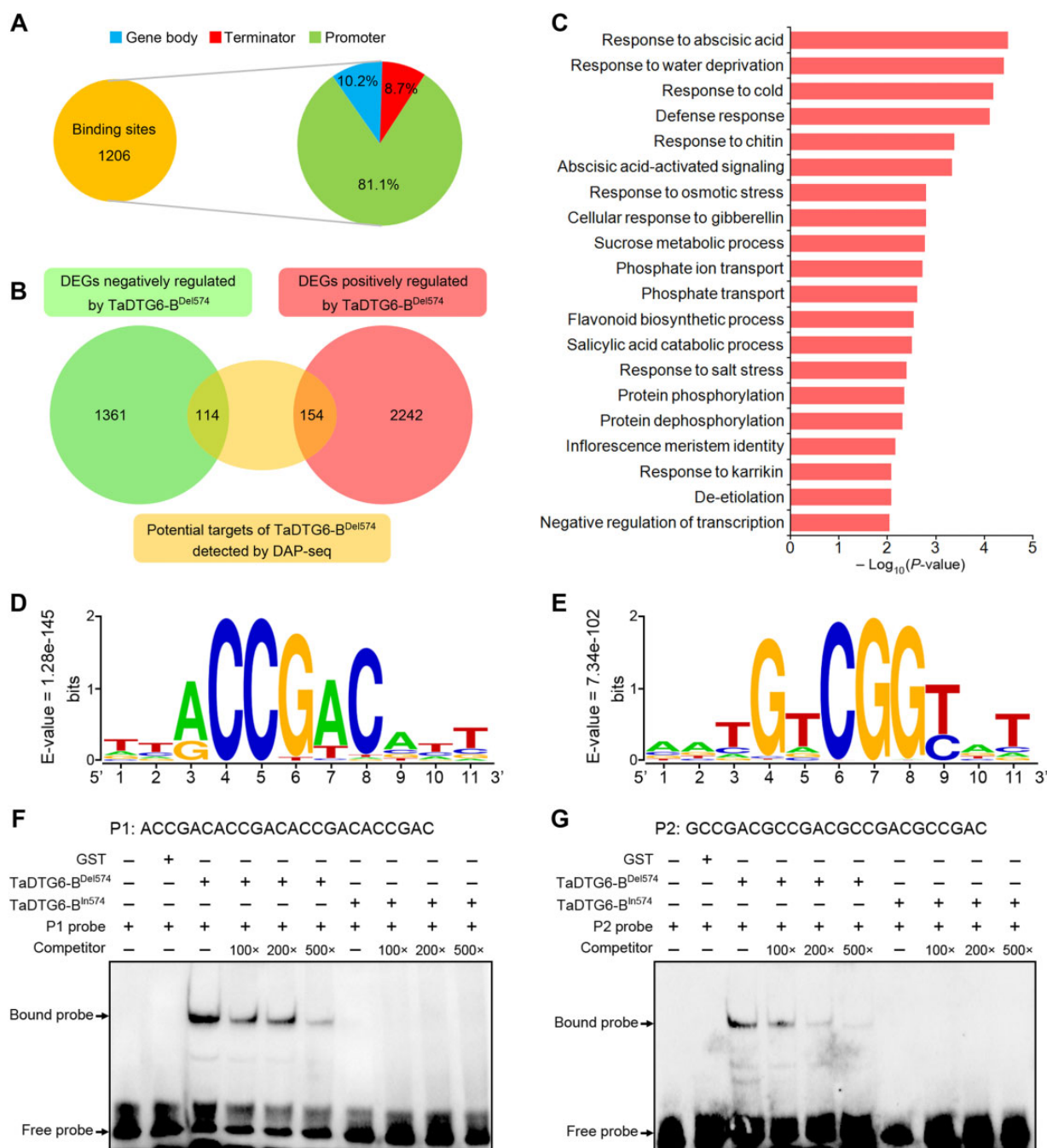
Figure 7 Genome-wide identification of TaDTG6-B^{Del574} binding sites and target genes. A, Distribution of the locations of predicted binding sites within target genes. Promoter was defined as the sequence within 2-kb upstream of the predicted transcriptional start site; terminator is the sequence within 2-kb downstream of the predicted transcription termination site; gene body consists of the 5′-UTR, exons, introns, and 3′-UTR. B, Venn diagram showing the extent of overlap between genes identified as DEGs by RNA-seq and potential TaDTG6-B targets, as determined by DAP-seq analysis. C, GO classification for DEGs with predicted TaDTG6-B^{Del574} binding sites. D and E, Identification of two motifs enriched in TaDTG6-B^{Del574} binding sequences using MEME software. F and G, EMSA showing that the DRE/CRT motifs ACCGAC (F) and GCCGAC (G) are required for TaDTG6-B^{Del574} binding to its targets. Recombinant GST-tagged TaDTG6-B^{Del574} and TaDTG6-B^{In574} were used in the EMSA, and GST was used as a control.

sites for the 268 target genes. This analysis resulted in the identification of two significantly enriched motifs for TaDTG6-B^{Del574}, with DRE/CRT cis-elements as the core motifs (ACCGAC/GCCGAC; Figure 7, D and E). To test whether TaDTG6-B^{Del574} and TaDTG6-B^{In574} directly bind to these DRE/CRT cis-elements in vitro, we conducted

electrophoretic mobility shift assays (EMSAs). We determined that recombinant GST-TaDTG6-B^{Del574} causes a slower migration of the labeled probes, which was effectively competed by incubation with unlabeled probes, indicative of strong and specific TaDTG6-B^{Del574} binding to DRE/CRT cis-elements. In contrast, we detected no binding between

the DRE/CRT cis-elements and TaDTG6-B^{In574} (Figure 7, F and G), suggesting that the TaDTG6-B^{In574} variant lacks the ability to regulate downstream target genes through these cis-elements. Consistently, our DAP-seq analysis only identified 184 TaDTG6-B^{In574} binding sites mapping to 47 target loci (Supplemental Data Set 15). However, all of these target genes encoded chloroplast-localized proteins, and showed no overlap with the target genes predicted for TaDTG6-B^{Del574}. This result indicated that TaDTG6-B^{In574} and TaDTG6-B^{Del574} may not share any nuclear target genes. Taken together, these results clearly indicated that the absence of the 26-bp insertion in the coding region of *TaDTG6-B* results in a gain of function of TaDTG6-B^{Del574} that entails direct binding to DRE/CRT cis-elements, and consequently, transcriptional regulation of stress-responsive genes to confer elevated drought tolerance in wheat seedlings.

TaDTG6-B^{Del574} enhances drought tolerance by modulating *TaPIF1* expression

Our RNA-seq analysis revealed that the expression of a *PIF* gene, TraesCS1A02G083000, is significantly upregulated in *TaDTG6-B^{Del574}* OE plants compared to WT (Supplemental Data Set 14). Phylogenetic analysis showed that the protein encoded by TraesCS1A02G083000 clusters with rice OsPIL15 (PIF-LIKE 15) and OsPIL16 (Todaka et al., 2012), as well as maize ZmPIF1 and ZmPIF3 (Gao et al., 2018a, 2018b; Supplemental Figure S13A), which led us to designate TraesCS1A02G083000 as *TaPIF1*. Subcellular localization assays using a TaPIF1-GFP fusion protein established that TaPIF1 localizes to the nucleus of wheat protoplasts transfected with the encoding construct (Supplemental Figure S13B). Previous studies have indicated that *TaPIF1* homologs contribute to enhanced water-use efficiency and drought tolerance via ABA pathway-induced stomatal closure (Kudo et al., 2017; Gao et al., 2018a, 2018b; Qiu et al., 2020), which suggested that *TaPIF1* could be an important target of TaDTG6-B for drought tolerance.
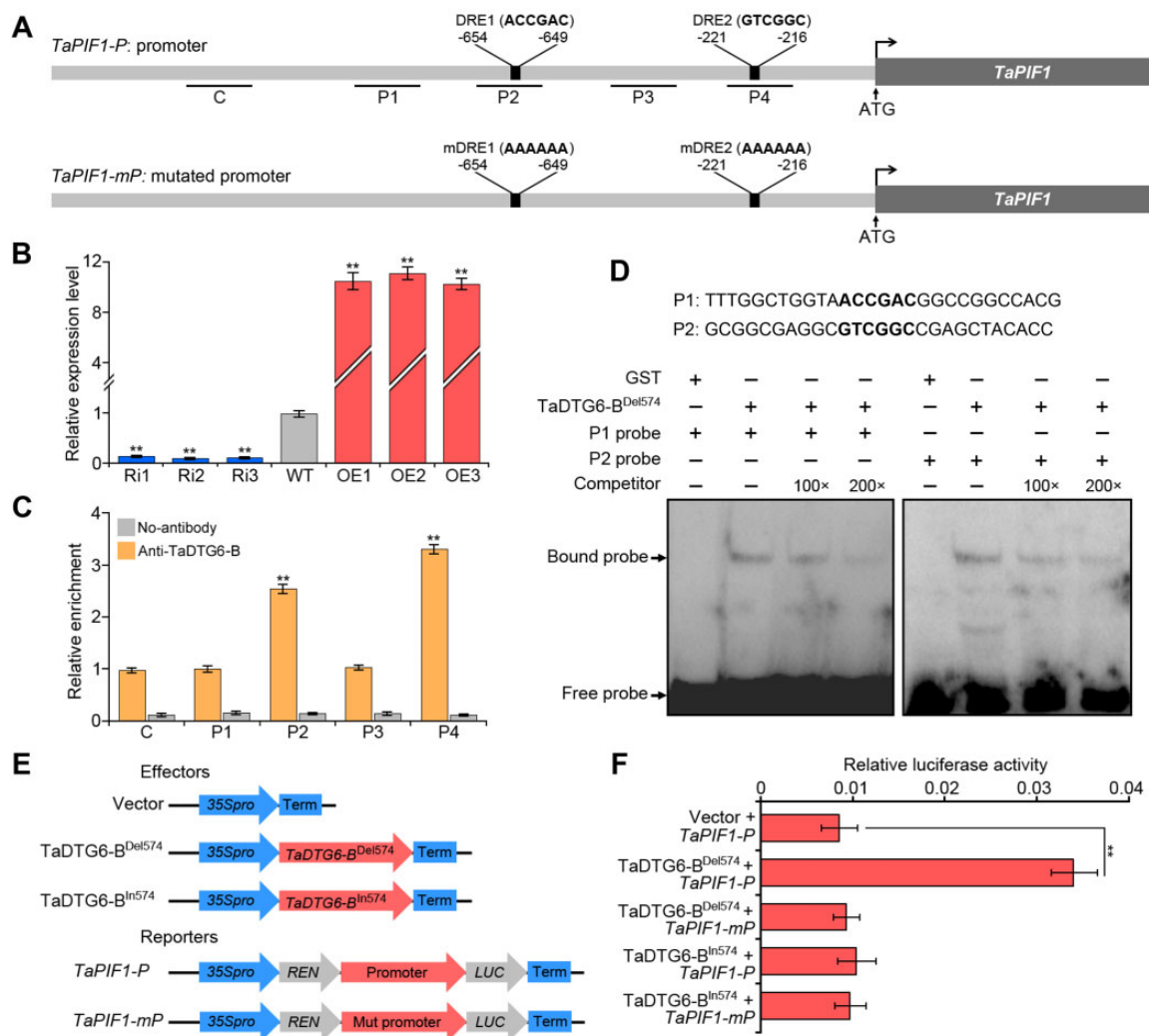
Indeed, an analysis of the *TaPIF1* promoter sequence detected the presence of two DRE/CRT cis-elements (ACCGAC and GTCGGC) (Figure 8A), and RT–qPCR analysis confirmed that *TaPIF1* expression is significantly higher in *TaDTG6-B^{Del574}* OE plants than in WT, but significantly lower in *TaDTG6-B* RNAi plants (Figure 8B). We also performed chromatin immunoprecipitation followed by quantitative PCR (ChIP-qPCR) assays using a series of promoter fragments containing or lacking the DRE/CRT cis-elements to test whether TaDTG6-B^{Del574} might directly bind to the *TaPIF1* promoter region in planta. We observed that TaDTG6-B^{Del574} is significantly enriched at *TaPIF1* promoter fragments containing the DRE/CRT cis-elements (Figure 8C). In addition, EMSAs demonstrated that TaDTG6-B can directly bind to the two DRE/CRT cis-elements in the *TaPIF1* promoter, in contrast to the lack of binding seen with the GST control protein (Figure 8D). Notably, we detected no binding between TaDTG6-B^{In574} and the *TaPIF1* promoter

fragments in EMSAs (Supplemental Figure S14), further indicating that the TaDTG6-B^{In574} variant lacks the ability to regulate downstream target genes through DRE/CRT cis-elements. We then used a transient expression system to assess whether this binding can indeed induce *TaPIF1* transcription in vivo. To this end, we generated a series of reporter constructs with the *LUC* reporter gene driven by *TaPIF1* promoters containing either intact (WT) or mutated DRE/CRT cis-elements. We then separately co-infiltrated these constructs into *Nicotiana benthamiana* leaves together with an effector construct overexpressing TaDTG6-B^{Del574} or the empty pGreenII 62-SK vector. Compared to the empty vector controls, the transient expression of TaDTG6-B^{Del574} resulted in significantly higher LUC activity driven by the intact *TaPIF1* promoter construct. However, disruption of the DRE/CRT cis-elements abolished TaDTG6-B^{Del574}-mediated transactivation of the *TaPIF1* promoter (Figure 8, E and F), indicating that TaDTG6-B^{Del574} positively regulates *TaPIF1* transcription.

To characterize TaPIF1 function in the wheat response to drought stress, we overexpressed *TaPIF1* under the control of the maize *Ubiquitin* promoter in wheat *cv*. Fielder. We first confirmed that *TaPIF1* transcript levels are in fact significantly higher in *Ubipro:TaPIF1* transgenic OE lines compared to WT plants (Figure 9A). Following drought stress imposed by water withholding, all transgenic OE lines exhibited significantly enhanced drought tolerance phenotypes compared to the WT (Figure 9, B and C). We also assayed the contents for proline, malondialdehyde (MDA), soluble sugars, and chlorophylls under well-watered and drought conditions. We detected no differences in these four physiological parameters between the WT and *Ubipro:TaPIF1* OE lines under well-watered conditions. In contrast, the contents for proline, soluble sugars, and chlorophylls were significantly higher, while MDA content was significantly lower in the OE lines compared to WT under drought stress conditions (Figure 9, D–G). Taken together, these results strongly indicate that the activation of *TaPIF1* expression can lead to greater drought tolerance in wheat seedlings, and thus illustrates a major mechanism by which TaDTG6-B^{Del574} regulates this phenotype.

Discussion

A better understanding of genotype–phenotype relationships will help guide the development of new drought-tolerant varieties. Here, we aimed to better understand the molecular mechanisms associated with the genetic polymorphisms underlying the variation in drought tolerance of wheat seedlings. To this end, we performed GWAS, in conjunction with candidate gene association analysis transgenic assays to reveal the significant association between an elite allele of a *DREB* gene, *TaDTG6-B*, and elevated drought tolerance in wheat seedlings (Figures 2, 3, and 6). In particular, our study provides three major discoveries surrounding wheat response to drought stress. First, we showed that the gain-of-function variant TaDTG6-B^{Del574} functions as a major

Figure 8 TaDTG6-B^{Del574} can directly induce *TaPIF1* transcription. A, Schematic diagram of the *TaPIF1* promoter (WT [intact] and mutated). The DRE/CRT cis-elements are indicated by black boxes. B, RT–qPCR analysis of relative *TaPIF1* expression levels in the WT, *Ubipro:TaDTG6-B*^{Del574} OE lines, and *TaDTG6-B* RNAi lines. C, ChIP-qPCR validation of TaDTG6-B^{Del574} binding sites in the *TaPIF1* promoter. The fragments used in ChIP-qPCR are indicated in (A). D, EMSA of TaDTG6-B^{Del574} binding to the DRE/CRT cis-elements in the *TaPIF1* promoter. Biotin-labeled probes were incubated with GST or GST-tagged TaDTG6-B^{Del574}. 100 × and 200 × unlabeled competitor fragments were added to evaluate binding specificity. E-F, TaDTG6-B increases *TaPIF1* promoter activity. *Nicotiana benthamiana* leaves were co-infiltrated with constructs encoding either TaDTG6-B^{Del574} or TaDTG6-B^{In574} and either intact or mutated *TaPIF1* promoter. The firefly LUC/REN ratio indicates the level of transcriptional activation of the different promoters by each respective effector construct. Values are means ± sd from at least three independent experiments; statistical significance was determined by two-sided Student's *t* test (**$P < 0.01$).

transcriptional regulator of stress-responsive genes, resulting in amelioration of drought tolerance in wheat seedlings. Second, we identified *TaPIF1* as a direct target of TaDTG6-B^{Del574} transcriptional regulation via binding to DRE/CRT promoter elements that increases drought tolerance. Last but not the least, *TaDTG6-B*^{Del574} is an optimal allele that could be utilized for molecular breeding to improve drought tolerance in wheat.

The discovery of allelic variants (e.g. SNPs or InDels) in functional genes coupled with analyses of their effects on phenotypes is a potentially useful strategy to elucidate their influence on the function of their encoded proteins for variety improvement (Hickey et al., 2019; Gao, 2021; Liang et al., 2021). In this work, we determined that a 26-bp InDel (InDel574) in the

coding region of *TaDTG6-B* results in major effects on the TaDTG6-B protein variants for the regulation of stress-responsive genes in wheat. Mechanistically, TaDTG6-B^{Del574} exhibited stronger transcriptional activation, broader-specificity protein interactions, and gain-of-function binding ability to DRE/CRT cis-elements compared to TaDTG6-B^{In574} resulting from the 26-bp insertion in TaDTG6-B (Figures 4, E, 5, 7, F and G). The ectopic expression of *TaDTG6-B*^{Del574} in Arabidopsis or transgenic overexpression in wheat resulted in significantly greater tolerance to drought stress, whereas the overexpression of *TaDTG6-B*^{In574} showed no phenotypic effects relative to the WT (Figure 6; Supplemental Figures S9 and S10). Furthermore, replacement of the *TaDTG6-B*^{In574} allele in drought-sensitive varieties with the *TaDTG6-B*^{Del574} allele significantly ameliorated
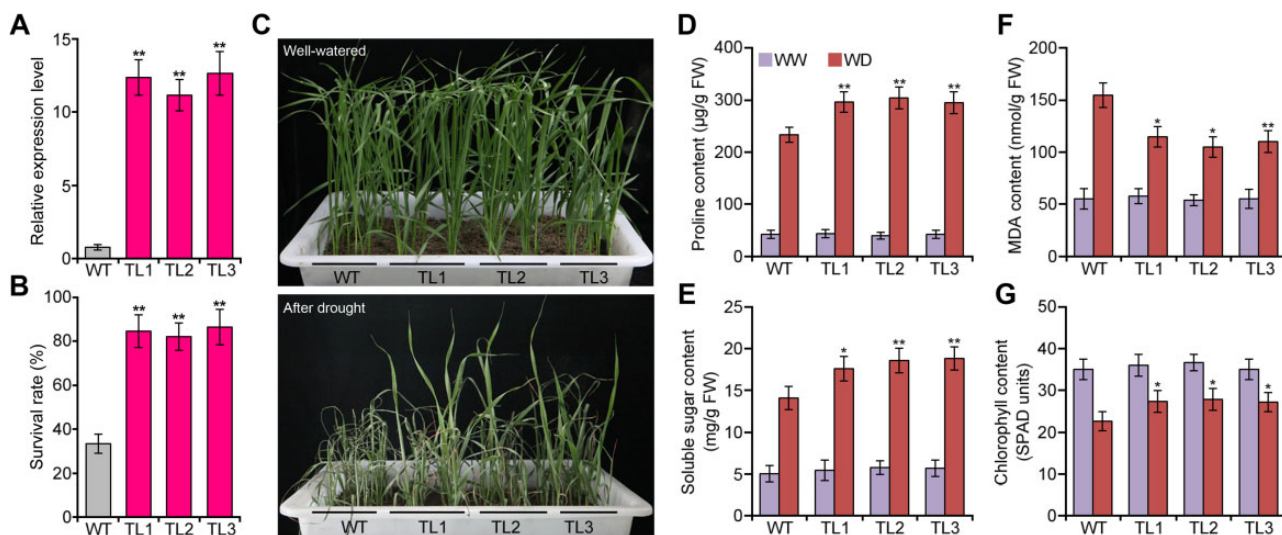
Figure 9 *TaPIF1* overexpression improves drought tolerance in transgenic wheat. A, Relative expression levels of *TaPIF1* in *Ubipro:TaPIF1* OE lines. B, SR in *Ubipro:TaPIF1* OE lines during drought treatment and recovery. C, Representative drought tolerance phenotypes in *Ubipro:TaPIF1* OE lines. Photographs were taken under well-watered conditions before drought treatment and after a 3-day recovery period with full irrigation post drought treatment. D–G, Physiological parameters of *Ubipro:TaPIF1* OE and WT plants under well-watered (WW) and water-deficit (WD) conditions. D, Proline contents. E, Soluble sugar contents. F, MDA contents. G, Chlorophylls contents. Values are means ± SD from at least three independent experiments; statistical significance was determined by two-sided Student's t test (*$P < 0.05$; **$P < 0.01$).

wheat drought tolerance (Figure 3, E–G), indicating that the introgression of elite alleles such as *TaDTG6-B*[Del574] provides an effective avenue for producing wheat varieties with stress tolerance (Tester and Langridge, 2010; Hu and Xiong, 2014). In addition, we established that the *TaDTG6-B*[Del574] elite allele might have arisen after the formation of hexaploid wheat and was retained in 44% of landraces, whereas we detected this allele in only 33% of the modern cultivars examined here (Figure 6J), suggesting that it has not been sufficiently utilized during modern wheat breeding programs. Taken together, the *TaDTG6-B*[Del574] allele can be a valuable target toward increasing drought tolerance for wheat germplasm improvement. However, further investigation is needed to determine how this 26-bp InDel could structurally alter TaDTG6-B to confer broader functionality in target gene recognition, as established by our results.

Despite the extensive knowledge on the biological functions of DREB TFs, their downstream signaling networks under drought stress conditions are still largely unknown. Here, transcriptome and DAP-seq analyses indicated that TaDTG6-B[Del574] may mediate stress tolerance by targeting genes involved in pathways related to water stress response, ABA response, cold response, and osmotic stress response (Figure 7, A–C; Supplemental Figures S11 and S12). Particularly, we found that TaDTG6-B[Del574] can bind to the *TaPIF1* promoter (Figure 8, A–D), which showed the highest upregulation of all targets regulated by TaDTG6-B. Further transient expression assays using the *LUC* reporter driven by the *TaPIF1* promoter revealed that TaDTG6-B is indeed a positive regulator of *TaPIF1* transcription (Figure 8, E and F). Although several studies have confirmed that the DREB-PIF module is an important regulator that optimizes plant growth and environmental adaptation (Kudo et al., 2017;

Dong et al., 2020; Jiang et al., 2020; Xu and Deng, 2020), the capacity of the DREB-PIF module underlying drought tolerance and crop improvement is largely unexplored. Recently, a growing body of evidence has pointed to PIFs as major players in the regulation of transcriptional response to drought stress in addition to their well-known roles in light responsive pathways (Leivar and Quail, 2011; Leivar and Monte, 2014). For instance, *ZmPIF1* and *ZmPIF3* overexpression in maize, or *OsPIL1* overexpression in rice, all significantly improved drought tolerance in their respective species (Todaka et al., 2012; Gao et al., 2018a, 2018b). In this study, we showed that *TaPIF1* overexpression resulted in improved drought tolerance in transgenic wheat seedlings (Figure 9, A–C). Although the molecular mechanisms by which plant growth and development are controlled by *TaPIF1* (or other *PIFs*) under stress conditions requires a more detailed study, our work revealed a positive regulatory role for the TaDTG6-B-*TaPIF1* module in adaptation to drought stress in wheat.

In addition, the three homoeologous genes found in the hexaploid wheat genome are frequently subject to independent and variable mechanisms of transcriptional and posttranscriptional regulation (Bottley et al., 2006; Shitsukawa et al., 2007; Hu et al., 2013; Kashkush et al., 2020; Gao et al., 2021; Liu et al., 2022). In this work, we found that the coding sequences of the *TaDTG6-A* and *TaDTG6-D* homoeologs carry the 26-bp insertion, similar to the *TaDTG6-B*[In574] allele (Supplemental Figure S7), suggesting that their encoded proteins also have similar activity to that of TaDTG6-B[In574]. Further sequence analysis revealed that this 26-bp insertion in the coding regions of *TaDTG6-A* and *TaDTG6-D* is conserved across wheat accessions, which led us to speculate
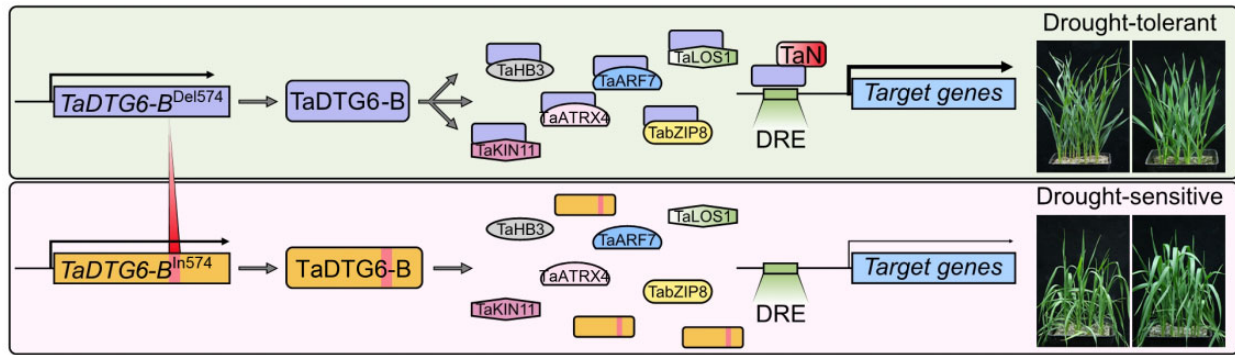
Figure 10 A working model for *TaDTG6-B*^{Del574} allele-mediated drought tolerance. Drought-tolerant wheat accessions carrying *TaDTG6-B*^{Del574} allele exhibit a stronger TaDTG6-B activity of transcriptional activation and protein interactions, and also have the ability to bind to DRE/CRT cis-elements to regulate stress-responsive gene expression, resulting in the improvement of drought tolerance. Drought-sensitive wheat accessions carrying the *TaDTG6-B*^{In574} allele have a lower TaDTG6-B activity of transcriptional activation and protein interactions, and cannot bind to DRE/CRT cis-elements, resulting in sensitivity to water deficiency.

that the *TaDTG6-B*^{Del574} allele represents an instance of functional divergence between this allele in drought-tolerant accessions and sensitive accessions carrying *TaDTG6-A*, *TaDTG6-B*^{In574}, and *TaDTG6-D*. This structural variant highlights a viable means of targeting specific homoeologs to improve agronomically desirable adaptive traits in polyploid crops (Van de Peer et al., 2017). Moreover, our results also revealed that the striking expansion of the DREB1 family (Supplemental Figure S6) was accompanied by loss of function in at least some of these wheat *DREB* genes.

Taken together, these results suggest a model for *TaDTG6-B* allelic variation in conferring drought response in wheat seedlings (Figure 10). Accordingly, tolerant wheat accessions carrying *TaDTG6-B*^{Del574} exhibit a stronger TaDTG6-B activity of transcriptional activation and protein interactions, and also have the ability to bind to DRE/CRT cis-elements to regulate stress-responsive gene expression, resulting in the improvement of drought tolerance. Drought-sensitive wheat accessions carrying the *TaDTG6-B*^{In574} allele have a lower TaDTG6-B activity of transcriptional activation and protein interactions, and cannot bind to DRE/CRT cis-elements, resulting in sensitivity to water deficiency. These collective results provide important breakthroughs in the scope of our understanding of how allelic variation in a transcription factor gene can drive phenotypic improvements in the quantitative agronomic traits of crops. In addition, our findings also hold major implications for the introgression of this *TaDTG6-B*^{Del574} allele into elite lines or recreating the 26-bp insertion allele by CRISPR/Cas9 (Clustered Regularly Interspaced Short Palindromic Repeats) to obtain gain-of-function mutants as two viable avenues for breeding improvement to drought tolerance traits.

Materials and methods

Drought tolerance evaluation of the wheat association panel
A GWAS for wheat drought-tolerant genes was performed by analyzing a wheat (*Triticum aestivum* L) diversity panel consisting of 430 wheat accessions (Supplemental Data Set 4). Plant drought tolerance of the different wheat accessions was recorded as previously described (Mao et al., 2020, 2022). Briefly, two cultivation pools (8.0 × 1.2 × 0.2 m, length × width × depth) were used for drought tolerance phenotyping assays, as measured by SR. This experiment was independently performed eight times, with each experiment consisting of two biological replicates of cultivation pools to facilitate estimation of random error. Each pool was divided into 430 plots containing a 4:1:2 (w/w/w) potting mixture of soil:vermiculite:water (total 1.4 tons), with a soil water content (SWC) of ~40%, as measured with a portable SU-LA soil moisture determinator instrument (Zhejiang TopuYunnong Technology Co., Ltd). All accessions were planted in random order with 12 plants per accession grown in each plot. Seedlings were grown in a greenhouse under 16 h of light (intensity of 20,000 lux) and 8 h of darkness in a 16°C/14°C (day/night) temperature cycle and a relative humidity of 60%. SWC measurements were collected every other day until leaves began to wilt, at which point SWC was measured every day. Re-watering was applied to allow the surviving plants to recover when clear wilting difference was observed; SRs were calculated 3 days after re-watering. Plants with green, living leaves were scored as surviving.

RNA-seq of the wheat association panel
For RNA-seq, at least five plants for each of the 430 accessions were cultivated as described above with full irrigation (i.e. no drought treatment). The second leaf was collected from each 3-week-old plant and leaves were pooled into a single sample per accession; the combined samples were flash-frozen in liquid nitrogen and stored at −80°C. Total RNA was extracted using TRIzol reagent (Invitrogen), and library preparation was conducted with a TruSeq paired-end mRNA-seq Illumina kit following the manufacturer's instructions. Samples were sequenced using a HiSeq X instrument to obtain 150-bp paired-end reads.

Read mapping and SNP calling

Quality control of raw sequencing reads was conducted using the FastQC software (http://www.bioinformatics.babraham.ac.uk/projects/fastqc). To obtain high-quality reads, the sequencing adapters and low-quality bases were removed from the raw RNA-seq data using Trimmomatic (Bolger et al., 2014) with default parameters. The remaining clean paired-end reads were mapped to the wheat reference genome (IWGSC v1.1) using HISAT2 v2.0.5 (Pertea et al., 2016) with the following parameters: -min-intronlen, 20; -max-intronlen, 10000; –dta-cufflinks. Only alignments with a mapping quality (MQ) >20 for single-end reads and concordant unique alignments for paired-end reads were kept for further analysis. The fragments per kilobase per million mapped fragments value for each gene in each sample was calculated using Cufflinks (Trapnell et al., 2012).

The genotype of each accession was determined using the Genome Analysis Toolkit (GATK v3.7; McKenna et al., 2010). Duplicate reads were flagged using the Picard package v1.115 MarkDuplicates (http://broadinstitute.github.io/picard/) and spliced reads were removed with the SplitNCigarReads package. SNPs were then called using the HaplotypeCaller package in GATK and mpileup package in SAMtools (Li et al., 2009; McKenna et al., 2010). The high confidence variants were selected according to the following criteria: quality depth (QD) $\geqslant 2.0$; ReadPosRankSum $\geqslant -8.0$; FS $\leqslant 60.0$; and Qual $\geqslant$ meanQual. Base quality scores were adjusted for the set of high confidence variants using the BaseRecalibrator package in GATK, and then the final round of SNP calling was performed with the HaplotypeCaller and GenotypeGVCFs packages in GATK. Missing genotypes were imputed using fastPHASE v1.3 (Scheet and Stephens, 2006). SNPs were then removed if the missing rate was $\geqslant 0.6$ or MAF < 0.05, resulting in a final set of 465,269 SNPs.

Population structure and LD of the association panel

The genotypes of the 430 accessions screened with the wheat 660K SNP array were also filtered using a missing rate < 0.6 and MAF $\geqslant 0.05$, resulting in a set of 397,761 SNPs. These SNPs were combined with the 465,269 high-quality SNPs obtained in the present study to generate a final set of 838,030 SNPs. The Genome Association and Prediction Integrated Tool (GAPIT; Lipka et al., 2012) was used to identify relationships between accessions and principal components via the efficient mixed model association (EMMA) method algorithm. TASSEL 5.0 (Bradbury et al., 2007) was used to calculate LD and nucleotide diversity. For each of the wheat subgenomes (A, B, and D), LD decay was calculated using the methods described by Wu et al. (2021). LD blocks were defined as groups of SNPs having an $r^2 \geqslant 0.5$, and block size was determined by calculating the physical distance between the outermost flanking SNPs.

GWAS

GAPIT was used to identify potential genome-wide associations for the 863,030 SNPs. Computational parameters were optimized using EMMA and a compressed mixed linear model; statistical performance was optimized using previously determined population parameters (Mao et al., 2022). SNP-based relationships between accessions were determined with EMMA. The top three principal components were used to control for population structure. Data visualization was conducted using the R package "CMplot" (https://github.com/YinLiLin/R-CMplot). The threshold to determine significant MTAs was set to 1.38×10^{-5}, which was determined by taking the average of 1/effective number of SNPs for the A, B, and D subgenomes. SNPs within a single LD block were combined into one associated genomic region. Annotation of genes in each region was conducted using the wheat reference genome (IWGSC v1.1), and relative expression of the associated genes was analyzed using data from the drought-stressed wheat *cv.* Chinese Spring.

TaDTG6-B gene association analysis

TaDTG6-B-based association mapping was conducted with 281 wheat accessions (Supplemental Data Set 7). The ~3.2-kb genomic region, consisting of the ~2.5-kb promoter, exons, 5′-UTR, and 3′-UTR sequences, was amplified and sequenced, using the primers listed in Supplemental Data Set 16. These sequences were assembled using ContigExpress in Vector NTI Advance 10 (Invitrogen) and aligned using MEGA version 6 (http://megasoftware.net/). Nucleotide polymorphisms, including InDels and SNPs (MAF $\geqslant 0.05$), were identified and further used to perform the MTAs with SR and to calculate pairwise LD using Tassel 5.0.

RNA isolation and RT–qPCR

Total RNA was extracted using TRIzol reagent (Invitrogen). After incubation with DNase I (TaKaRa), first-strand cDNA was generated from 1-μg template RNA for each sample in a total reaction volume of 20 μL using a Clontech reverse transcription kit. qPCR was conducted for each sample in a total reaction volume of 10 μL comprised 1-μL cDNA, 4-μL 0.2-mM forward and reverse primers (Supplemental Data Set 16), and 5-μL SYBR Premix Ex Taq master mix (TaKaRa). An ABI Step One System (Applied Biosystems) thermocycler was used for amplification with the following program: 10-min initial denaturation, 95°C, then 40 cycles of 15 s at 95°C and 30 s at 60°C. Relative gene expression was calculated with the $2^{-\Delta\Delta Ct}$ method (Livak and Schmittgen, 2001) using *TaActin1* as an internal control gene. qPCR was performed as technical triplicates per sample. Three biological replicates were performed, with similar results; the results from one replicate are shown in the figures.

Subcellular localization

For subcellular localization assays, the coding sequences of *TaDTG6-A*, *TaDTG6-B*^{Del574}, *TaDTG6-B*^{In574}, *TaDTG6-D*, and *TaPIF1* lacking stop codons were cloned into the pJIT163:GFP expression vector (Supplemental Data Set 16),

with transcription driven by the CaMV 35S promoter. These five constructs and the empty vector were then separately transformed into wheat mesophyll protoplasts using polyethylene glycol-mediated transformation as described by Yoo et al (2007). After 18 h of incubation for 23°C in the dark, fluorescence was visualized using a confocal microscope (FluoView FV300, Olympus, Japan) and quantified using the image analysis software provided by the manufacturer. For eGFP, the laser wavelength for excitation was 488 nm, and the emission was collected from 500 to 540 nm. For chlorophyll autofluorescence, the laser wavelength for excitation was 640 nm, and the emission was collected from 650 to 750 nm. For laser intensity, the Acousto-Optical Tunable Filter was adjusted to 1%–3%, and the Photomultiplier Tube voltage was adjusted to 400–700 in different experiments. The gain value of all lasers was set to the default value of 1,000.

Transactivation activity assay

Transactivation activity assays were conducted using yeast (*Saccharomyces cerevisiae* strain AH109) and *N. benthamiana* leaves. For yeast, plasmids were constructed by cloning the full-length coding sequences of *TaDTG6-A*, *TaDTG6-B*^{Del574}, *TaDTG6-B*^{In574}, and *TaDTG6-D* and truncated fragments of *TaDTG6-B*^{Del574} and *TaDTG6-B*^{In574} into the pGBKT7 vector and transformed into yeast (Supplemental Data Set 16). All yeast transformants were selected based on growth on synthetic defined (SD) medium lacking tryptophan (SD –Trp). PCR-verified transformants were then plated onto SD medium lacking tryptophan, histidine, and adenine and containing 5-bromo-4-chloro-3-indolyl-α-D-galactopyranoside acid (SD –Trp –His –Ade + X-α-gal). After 3–6 days of incubation at 30°C, growth rates were compared between corresponding colonies on the two media.

For assays in *N. benthamiana*, the coding sequences of *TaDTG6-A*, *TaDTG6-B*^{Del574}, *TaDTG6-B*^{In574}, and *TaDTG6-D* were cloned into the reconstructed GAL4-DBD vector to serve as effectors. The double reporter vector includes a GAL4 DNA consensus binding site derived from the yeast *GAL4* gene upstream of firefly luciferase (*GAL4 UAS:LUC*) and a Renilla (*REN*) gene as internal control driven by the 35S promoter. The effector and reporter plasmids were then co-infiltrated into *N. benthamiana* leaves. The LUC and REN luciferase activities were assayed using dual luciferase assay kits (Promega, Madison, WI, USA). Three replicates were carried out for each sample. All primers used for cloning are listed in Supplemental Data Set 16.

Wheat transformation and drought tolerance assay

TaDTG6-B knockdown and OE lines were generated for drought tolerance assays. For knockdown by RNAi, a 204-bp fragment of the *TaDTG6-B* coding sequence was synthesized and cloned in both the sense and antisense orientations on either side of the 508-bp intron 6 from rice (*Oryza sativa*) zinc-finger type family protein gene (Cui et al., 2019). The resulting DNA fragment was then inserted into the pWMB110 vector harboring the maize *Ubiquitin* promoter.

For overexpression, the coding sequences of *TaDTG6-B*^{Del574}, *TaDTG6-B*^{In574}, and *TaPIF1* were cloned into the pCAMBIA3301 vector, also driven by the maize *Ubiquitin* promoter. Agrobacterium (*Agrobacterium tumefaciens*)-mediated transformation was used to generate independent transgenic lines of each construct in the wheat *cv.* Fielder background, as described by Ishida et al. (2015). Transgene-positive plants were determined in T_0, T_1, and T_2 generations by PCR amplification of the transgene using specific primers (Supplemental Data Set 14) for the transgenic vectors. Transformed plants were screened and phenotyped in response to drought stress as described previously (Mao et al., 2020, 2022). Briefly, T_3 transgene-positive and WT plants were planted together in enriched soil (soil and vermiculite in a ratio of 3:1, w/w), and grown under 16 h of light (intensity of 20,000 lux) and 8 h of darkness under a 16–C/14°C temperature cycle and a relative humidity of 60% conditions in a greenhouse. Drought treatment was applied to soil-grown plants at the three-leaf seedling stage by withholding water. After ~25 days of water withholding, watering was resumed to allow plants to recover. The number of surviving plants was recorded 3 days later. At least 18 plants of each line were compared in each test and statistical analyses were based on data obtained from four independent experiments. All primers used for cloning are listed in Supplemental Data Set 16.

Introgression of the *TaDTG6-B* elite allele

The drought-tolerant wheat *cv.* Jinmai47 was separately crossed with two drought-sensitive cultivars, GLUYAS EARLY and Yangmai13. Heterozygous progeny was backcrossed with the drought-sensitive cultivars to produce the BC_4F_1 generation (InDel574 was genotyped at each generation). The BC_4F_1 plants were then self-pollinated to obtain BC_4F_2 plants for analysis. The morphological and drought stress phenotypes were compared between NILs that were homozygous for either the tolerant or sensitive (In574) allele of *TaDTG6-B*.

Illumina library preparation and DAP-seq

Genomic DNA libraries were prepared as described by Bartlett et al (2017). The coding sequences of *TaDTG6-B* and *TaDTG6-B*^{In574} from wheat *cv.* Chinese Spring and GLUYAS EARLY were cloned into the pFN19K HaloTag T7 SP6 Flexi vector and produced using a TNT SP6 Coupled Wheat Germ Extract System (Promega, Madison, WI, USA). Magne Halo Tag Beads (Promega) were used to purify and capture the produced protein. Recombinant-purified GST-TaDTG6-B^{Del574} protein was bound to MagneGST beads (Promega). Five to 20 μg of purified protein (corresponding to 20 μL per sample) was incubated with 400 μL 1 × phosphate-buffered saline (PBS, pH 8.5) and 25-μL Magne Halo Tag beads for 1 h at room temperature with gentle mixing using a rotating shaker. Beads were washed four times in 1 × PBS with 0.005% (v/v) NP40, then resuspended in 100 μL 1 × PBS. Genomic DNA (1 g DNA in 60 μL 1 × PBS) was added to the protein-bound beads, and

then shaken for 1 h. Afterwards, the beads were washed four times in 1 × PBS with 0.005% (v/v) NP40, followed by two washes in 1 × PBS. After transferring beads to 25-μL elution buffer in fresh tubes, DNA was extracted by boiling at 98°C for 10 min.

Eluted samples were enriched then tagged using dual-indexed multiplexing barcodes. The pooled tagged samples were sequenced using an Illumina HiSeq 2500 to generate 150-bp single-end reads. Adapters were removed with Trimmomatic (Bolger et al., 2014) and the resulting reads were mapped to the wheat reference genome (IWGSC v1.1). Peaks indicating protein binding were identified using GEM v2.5 (Guo et al., 2012). The GST-HALO negative control was used to control for the background using an FDR <0.001. Motifs with the highest levels of protein binding were identified with MEME-CHIP (Machanick and Bailey, 2011) using 200 bp (100-bp upstream and downstream) surrounding each peak.

RNA-seq analysis of transgenic wheat
RNA-seq was conducted using three biological replicates of the RNA samples collected from the leaves of 30-day-old *TaDTG6-B*^{Del574} transgenic and WT plants under well-watered and drought conditions. Total RNA was isolated according to the manufacturer's instructions for TRIzol reagent (Invitrogen). RNA quality and concentration were determined with an Agilent 2100 Bioanalyzer (Agilent Technologies) and an Agilent RNA 6000 Nano Kit. Sequencing libraries were prepared following the manufacturer's protocols for Illumina TruSeq RNA Sample Preparation (v2) and sequenced with an Illumina HiSeq 2500 platform. Data were processed and analyzed as described above. Genes with an absolute Log_2 value (fold-change) >1 and P <0.001 were classified as DEGs. GO term enrichment analysis of the upregulated and downregulated DEGs was conducted using the GOseq package in R (Young et al., 2010).

Antibody preparation against TaDTG6-B and immunoblotting
To prepare antibodies against TaDTG6-B, the sequence encoding the N terminus of TaDTG6-B was ligated into the pET-28a(+) vector (Supplemental Data Set 16), then transformed into *Escherichia coli* BL21 (DE3) for purification. Production of the recombinant fusion protein was induced by 6 h incubation with 1.0-mM isopropyl-β-D-thiogalactoside (IPTG; Promega) at 37°C. Ni2$^+$-nitrilotriacetate (Ni-NTA) agarose (Qiagen, Hilden, Germany) was used for affinity purification of His-TaDTG6-B following the manufacturer's instructions. Antibody was then generated by Wuhan GeneCreate Biological Engineering Co., Ltd, by immunizing rabbits with His-TaDTG6-B protein, followed by affinity purification from serum. For IB, phenol extraction and ammonium acetate–methanol precipitation were used to isolate the protein fraction from transgenic OE and RNAi wheat lines. Protein samples were mixed with an equal volume of 2 × protein loading buffer and boiled at 95°C for 10 min.

The extracts were centrifuged at 12,000g for 5 min at 4°C, and the proteins in the extracts were separated by sodium dodecyl sulfate–polyacrylamide gel electrophoresis. PageRuler prestained Protein Ladder (Thermo Fisher Scientific, Waltham, MA, USA) was used as size standards. The proteins were transferred to PVDF membranes and detected with antibodies against Actin (ABclonal, Woburn, MA, USA; AC009). Actin served as the loading control.

ChIP-qPCR analysis
ChIP assays were performed using 20-day-old *Ubipro:TaDTG6-B*^{Del574} transgenic wheat plants cultivated under the hydroponic conditions described above, using methods described in previous studies (Bowler et al., 2004). Crosslinking was conducted by a 10-min incubation in 1% (w/v) formaldehyde under vacuum, followed by tissue maceration in liquid nitrogen for nuclei isolation. The chromatin was sonicated into DNA fragments of 200 bp on average using an ultrasonic cell crusher (JY92-IIN), power settings of 15%, 3 s on and 2 s off, crushing for 20 min and the antibody against TaDTG6-B was used for chromatin immunoprecipitation. The precipitated DNA was then amplified by qPCR. Each experiment was performed as three independent replicates. All primers used for ChIP-qPCR are listed in Supplemental Data Set 16.

EMSA
The coding sequences of *TaDTG6-B*^{Del574} and *TaDTG6-B*^{In574} from wheat *cv*. Chinese Spring and GLUYAS EARLY were cloned into the pGEX4T-1 vector (Supplemental Data Set 16), respectively. *Escherichia coli* strain Rosetta (DE3, Promega) was transformed with the resulting constructs. The recombinant proteins were induced at OD (optical density)$_{600}$ = 0.6 using 0.1-mM IPTG with overnight incubation at 16°C, *E. coli* cells were broken by an ultrasonic cell crusher (JY92-IIN), with power set to 10%, 3 s on and 2 s off, crushing for 10 min until the bacterial suspension appeared clear. The GST fusion proteins were purified using GST-Sefinose resin (Promega) according to the manufacturer's instructions. EMSA was then conducted using the LightShift Chemiluminescent EMSA Kit (Thermo Fisher Scientific, Waltham, MA, USA) following the manufacturer's instructions.

Dual-luciferase transcriptional activity assay
Dual-luciferase transcriptional activity assays were conducted as described by Gao et al. (2021). The reporter construct was generated by cloning the ~1.5-kb promoter region of the *TaPIF1* gene from the wheat *cv*. Chinese Spring into the pGreenII 0800-LUC vector (Promega); the effector constructs were generated by cloning the coding sequences of *TaDTG6-B* and *TaDTG6-B*^{In574} into the pGreenII 62-SK vector (Promega) under the control of the CaMV 35S promoter (Supplemental Data Set 16). Agrobacterium strain GV3101 was transformed with each construct separately, and the resulting Agrobacterium colonies were used to co-infiltrate 4-week-old *N. benthamiana* leaves with the reporter and effector plasmids. Luciferase levels were measured using a Dual-Luciferase Reporter Assay System (Promega) following

the manufacturer's instructions. Normalized data are presented as the ratio of luminescent signal intensity for reporter versus internal control reporter (*35Spro:REN*) from three independent biological samples.

Y2H assay

For Y2H assays, the coding sequences of cofactors were cloned into the pGADT7 vector, and the coding sequences of *TaDTG6-B*^{Del574} and *TaDTG6-B*^{In574} were cloned into the pGBKT7 vector (Supplemental Data Set 16). The lithium acetate method was used to transform the resulting plasmids into yeast strain AH109. The transformed yeast strains were grown on double dropout (SD –L–T) medium, as per instructions in the manual (Clontech), and plates with quadruple dropout medium (SD –L–T–A–H) with X-gal overlay were used, with colonies harboring p53 as positive control to screen for potential interactions.

LCI assay

For split luciferase complementation assays, the coding sequences of cofactors were amplified and ligated into the JW772-35S-CLuc vector for expression of the C-terminal luciferase fusion protein (*cLUC*). The full-length coding sequences of *TaDTG6-B*^{Del574} and *TaDTG6-B*^{In574} were cloned into the JW771-35S-NLuc vector, which harbors the sequence encoding the N-terminal of luciferase fusion protein (nLUC; Supplemental Data Set 16). *Nicotiana benthamiana* leaves were co-infiltrated via Agrobacterium-mediated infiltration. The infiltrated plants were incubated in a growth chamber for 72–84 h at 28°C, after which the sites used for Agrobacterium infiltration were injected with 1-µM D-luciferin (Beetle luciferin, Promega). Luminescence signals were observed through a low-light cooled charge-coupled device imaging apparatus (Tanon 5200) after 40–48 h of cultivation. Three replicates were performed, with similar results; the results from one replicate are shown in the figures.

Statistical analysis

Two group comparisons between the control and experimental groups were performed using two-tailed t tests. Means were considered significantly different based on a threshold values of $P < 0.05$ and $P < 0.01$, as indicated by * and **, respectively. One-way analysis of variance was conducted using R with default parameters. Details are shown in Supplemental Data Set 17.

Accession numbers

The RNA-seq reads for 430 wheat accessions have been deposited in the Genome Sequence Archive in BIG Data Center, Beijing Institute of Genomics (BIG), Chinese Academy of Science, and are publicly accessible at https://ngdc.cncb.ac.cn/gsa under accession number CRA005898. The RNA-seq reads have also been deposited in the National Center for Biotechnology Information under project numbers PRJNA795836 (accession number SRP367570; SRA runs SRR18614846–SRR18615275) for the 430 wheat accessions and PRJNA795838 (accession number SRP376773;

SRR19370956–SRR19370963) for the *TaDTG6-B* transgenic lines. The RNA-seq data for Chinese Spring under normal growth conditions (SRR19854967 and SRR19854968) and drought conditions (SRR19854977 and SRR19854978 for 3 h under drought treatment, SRR19854973 and SRR19854974 for 12 h under drought treatment) were deposited at the NCBI SRA. The DAP-seq data of TaDTG6-B^{In574} and TaDTG6-B^{Del574} were deposited under project number PRJNA795838 (SRR20725205–SRR20725208).

TaDTG6-A (TraesCS2A02G399500), *TaDTG6-B* (TraesCS2B02G417500), *TaDTG6-D* (TraesCS2D02G397000), *TaNAC071-A* (TraesCS4A02G219700), *TaMYBL1* (TraesCS6D02G211100), *TaPIF1* (TraesCS1A02G083000), *OsDREB1E* (Os04g0572400), *OsPIL15* (Os01g0286100), *OsPIL16* (Os05g0139100), *ZmDREB1.10* (Zm00001eb073550), *ZmPIF1* (Zm00001eb129520), *ZmPIF3* (Zm00001eb332400).

Supplemental data

The following materials are available in the online version of this article.

Supplemental Figure S1. Distribution of SNPs in the association panel.

Supplemental Figure S2. Population structure and LD of the association panel.

Supplemental Figure S3. GO of 284 candidate genes identified by GWAS.

Supplemental Figure S4. Expression patterns of the nine candidate genes.

Supplemental Figure S5. The drought-tolerant allele of *TaDTG6-B* co-segregates with drought tolerance in two BC$_4$F$_2$ populations of wheat.

Supplemental Figure S6. Phylogenetic analysis of DREB proteins from Arabidopsis, rice, maize, and wheat.

Supplemental Figure S7. Alignment of *TaDTG6-A*, *TaDTG6-B*^{Del574}, *TaDTG6-B*^{In574}, and *TaDTG6-D* coding region sequences.

Supplemental Figure S8. GO of 69 potential cofactors of TaDTG6-B^{Del574} identified by Y2H.

Supplemental Figure S9. Drought tolerance of the *35S:TaDTG6-B*^{In574} and *35S:TaDTG6-B*^{Del574} transgenic Arabidopsis lines.

Supplemental Figure S10. Phenotype of *Ubipro:TaDTG6-B*^{Del574} transgenic and WT plants at the adult stage under well-watered conditions.

Supplemental Figure S11. Transcriptome analysis of *Ubipro:TaDTG6-B*^{Del574} transgenic wheat under well-watered conditions.

Supplemental Figure S12. Transcriptome analysis of *Ubipro:TaDTG6-B*^{Del574} transgenic wheat under water-deficit conditions.

Supplemental Figure S13. Phylogenetic analysis and subcellular localization of TaPIF1.

Supplemental Figure S14. EMSA test of TaDTG6-B^{In574} binding to the DRE/CRT cis-elements in the *TaPIF1* promoter.

Supplemental Data Set 1. Statistics of aligned reads identified by RNA sequencing in 430 wheat accessions.

Supplemental Data Set 2. A summary of the genetic diversity found in the sub-genomes and chromosomes of 430 wheat accessions, and evaluation of the effective number of independent SNPs, including suggested *P*-value thresholds.

Supplemental Data Set 3. Detailed information of LD blocks referred to Supplemental Figure S1E.

Supplemental Data Set 4. The 430 wheat accessions and their drought tolerance phenotype (SR) used for GWAS.

Supplemental Data Set 5. Information of significant SNP-trait associations.

Supplemental Data Set 6. Annotated genes within the genomic regions associated with SR.

Supplemental Data Set 7. Genetic variation in the *TaDTG6-B* genomic region and their association with wheat drought tolerance.

Supplemental Data Set 8. Potential TaDTG6-B^{Del574} cofactors identified in this study.

Supplemental Data Set 9. Potential TaDTG6-B^{In574} cofactors identified in this study.

Supplemental Data Set 10. List of 150 wheat landraces used for genotyping InDel574 polymorphism marker.

Supplemental Data Set 11. List of 300 modern wheat cultivars used for genotyping InDel574 polymorphism marker.

Supplemental Data Set 12. Significantly upregulated or downregulated genes in *Ubipro:TaDTG6-B*^{Del574} transgenic wheat grown under well-watered conditions.

Supplemental Data Set 13. Significantly upregulated or downregulated genes in *Ubipro:TaDTG6-B*^{Del574} transgenic wheat grown under drought conditions.

Supplemental Data Set 14. List of genes bound and regulated by TaDTG6-B^{Del574}.

Supplemental Data Set 15. List of target sites and potential genes bound and regulated by TaDTG6-B^{In574}.

Supplemental Data Set 16. Primers used for gene expression and vector construction.

Supplemental Data Set 17. Statistical analysis results for each figure.

Supplemental File S1. Protein sequences for the phylogenetic tree shown in Supplemental Figure S6.

Supplemental File S2. Newick format of the phylogenetic tree of Supplemental Figure S6.

Supplemental File S3. Protein sequences of the phylogenetic tree shown in Supplemental Figure S13.

Supplemental File S4. Newick format of the phylogenetic tree of Supplemental Figure S13.

References

Abberton M, Batley J, Bentley A, Bryant J, Cai H, Cockram J, de Oliveira AC, Cseke LJ, Dempewolf H, De Pace C, et al. (2016) Global agricultural intensification during climate change: a role for genomics. Plant Biotechnol J **14**: 1095–1098

Agarwal PK, Gupta K, Lopato S, Agarwal P (2017) Dehydration responsive element binding transcription factors and their applications for the engineering of stress tolerance. J Exp Bot **68**: 2135–2148

Ault TR (2020) On the essentials of drought in a changing climate. Science **368**: 256–260

Bailey-Serres J, Parker JE, Ainsworth EA, Oldroyd GED, Schroeder JI (2019) Genetic strategies for improving crop yields. Nature **575**: 109–118

Bartlett A, O'Malley RC, Huang SC, Galli M, Nery JR, Gallavotti A, Ecker JR (2017) Mapping genome-wide transcription-factor binding sites using DAP-seq. Nat Protoc **12**: 1659–1672

Barrero RA, Bellgard M, Zhang X (2011) Diverse approaches to achieving grain yield in wheat. Funct Integr Genomics **11**: 37–48

Blein-Nicolas M, Negro SS, Balliau T, Welcker C, Cabrera-Bosquet L, Nicolas SD, Charcosset A, Zivy M (2020) A systems genetics approach reveals environment-dependent associations between SNPs, protein coexpression, and drought-related traits in maize. Genome Res **30**: 1593–1604

Bolger AM, Lohse M, Usadel B (2014) Trimmomatic: a flexible trimmer for Illumina sequence data. Bioinformatics **30**: 2114–2120

Bottley A, Xia GM, Koebner RM (2006) Homoeologous gene silencing in hexaploid wheat. Plant J **47**: 897–906

Bowler C, Benvenuto G, Laflamme P, Molino D, Probst AV, Tariq M, Paszkowski J (2004) Chromatin techniques for plant cells. Plant J **39**: 776–789

Bradbury PJ, Zhang Z, Kroon DE, Casstevens TM, Ramdoss Y, Buckler ES (2007) TASSEL: software for association mapping of complex traits in diverse samples. Bioinformatics **23**: 2633–2635

Cui XY, Gao Y, Guo J, Yu TF, Zheng WJ, Liu YW, Chen J, Xu ZS, Ma YZ (2019) BES/BZR transcription factor TaBZR2 positively regulates drought responses by activation of *TaGST1*. Plant Physiol **180**: 605–620

Daryanto S, Wang L, Jacinthe PA (2016) Global synthesis of drought effects on maize and wheat production. PLoS One **11**: e0156362.

Dong X, Yan Y, Jiang B, Shi Y, Jia Y, Cheng J, Shi Y, Kang J, Li H, Zhang D, et al. (2020) The cold response regulator CBF1 promotes *Arabidopsis* hypocotyl growth at ambient temperatures. EMBO J **39**: e103630

Fu J, Cheng Y, Linghu J, Yang X, Kang L, Zhang Z, Zhang J, He C, Du X, Peng Z, et al. (2013) RNA sequencing reveals the complex regulatory network in the maize kernel. Nat Commun **4**: 2832

Gao C (2021) Genome engineering for crop improvement and future agriculture. Cell **184**: 1621–1635

Gao Y, An K, Guo W, Chen Y, Zhang R, Zhang X, Chang S, Rossi V, Jin F, Cao X, et al. (2021) The endosperm-specific transcription factor TaNAC019 regulates glutenin and starch accumulation and its elite allele improves wheat grain quality. Plant Cell 33: 603–622

Gao Y, Wu M, Zhang M, Jiang W, Liang E, Zhang D, Zhang C, Xiao N, Chen J (2018) Roles of a maize phytochrome-interacting factors protein ZmPIF3 in regulation of drought stress responses by controlling stomatal closure in transgenic rice without yield penalty. Plant Mol Biol 97: 311–323

Gao Y, Wu M, Zhang M, Jiang W, Ren X, Liang E, Zhang D, Zhang C, Xiao N, Li Y, et al. (2018) A maize phytochrome-interacting factors protein ZmPIF1 enhances drought tolerance by inducing stomatal closure and improves grain yield in *Oryza sativa*. Plant Biotechnol J 16: 1375–1387

Gaxiola RA, Li J, Undurraga S, Dang LM, Allen GJ, Alper SL, Fink GR (2001) Drought- and salt-tolerant plants result from overexpression of the AVP1 H + -pump. Proc Natl Acad Sci USA 98: 11444–11449

Gómez LD, Gilday A, Feil R, Lunn JE, Graham IA (2010) AtTPS1-mediated trehalose 6-phosphate synthesis is essential for embryogenic and vegetative growth and responsiveness to ABA in germinating seeds and stomatal guard cells. Plant J 64: 1–13

Gong Z, Xiong L, Shi H, Yang S, Herrera-Estrella LR, Xu G, Chao DY, Li J, Wang PY, Qin F, et al. (2020) Plant abiotic stress response and nutrient use efficiency. Sci China Life Sci 63: 635–674

Guo Y, Mahony S, Gifford DK (2012) High resolution genome wide binding event finding and motif discovery reveals transcription factor spatial binding constraints. PLoS Comput Biol 8: e1002638

Guo Z, Yang W, Chang Y, Ma X, Tu H, Xiong F, Jiang N, Feng H, Huang C, Yang P, et al. (2018) Genome-wide association studies of image traits reveal genetic architecture of drought resistance in rice. Mol Plant 11: 789–805

Gupta A, Rico-Medina A, Caño-Delgado AI (2020) The physiology of plant responses to drought. Science 368: 266–269

Hemsley PA, Kemp AC, Grierson CS (2005) The TIP GROWTH DEFECTIVE1 S-acyl transferase regulates plant cell growth in *Arabidopsis*. Plant Cell 17: 2554–2563

Hickey LT, N Hafeez A, Robinson H, Jackson SA, Leal-Bertioli SCM, Tester M, Gao C, Godwin ID, Hayes BJ, Wulff BBH (2019) Breeding crops to feed 10 billion. Nat Biotechnol 37: 744–754

Hu H, Xiong L (2014) Genetic engineering and breeding of drought-resistant crops. Annu Rev Plant Biol 65: 715–741

Hu Z, Han Z, Song N, Chai L, Yao Y, Peng H, Ni Z, Sun Q (2013) Epigenetic modification contributes to the expression divergence of three *TaEXPA1* homoeologs in hexaploid wheat (*Triticum aestivum*). New Phytol 197: 1344–1352

Ishida Y, Tsunashima M, Hiei Y, Komari T (2015) Wheat (*Triticum aestivum* L.) transformation using immature embryos. Methods Mol Biol 1223: 189–198

IWGSC (2018) Shifting the limits in wheat research and breeding using a fully annotated reference genome. Science 361: eaar7191

Jiang B, Shi Y, Peng Y, Jia Y, Yan Y, Dong X, Li H, Dong J, Li J, Gong Z, et al. (2020) Cold-induced CBF-PIF3 interaction enhances freezing tolerance by stabilizing the phyB thermosensor in *Arabidopsis*. Mol Plant 13: 894–906

Kashkush K, Feldman M, Levy AA (2020) Gene loss, silencing and activation in a newly synthesized wheat allotetraploid. Genetics 160: 1651–1659

Kasuga M, Liu Q, Miura S, Yamaguchi-Shinozaki K, Shinozaki K (1999) Improving plant drought, salt, and freezing tolerance by gene transfer of a single stress-inducible transcription factor. Nat Biotechnol 17: 287–291

Kirch HH, Nair A, Bartels D (2001) Novel ABA- and dehydration-inducible aldehyde dehydrogenase genes isolated from the resurrection plant *Craterostigma plantagineum* and *Arabidopsis thaliana*. Plant J 28: 555–567

Kudo M, Kidokoro S, Yoshida T, Mizoi J, Todaka D, Fernie AR, Shinozaki K, Yamaguchi-Shinozaki K (2017) Double

overexpression of DREB and PIF transcription factors improves drought stress tolerance and cell elongation in transgenic plants. Plant Biotechnol J 15: 458–471

Langridge P, Reynolds M (2021) Breeding for drought and heat tolerance in wheat. Theor Appl Genet 134: 1753–1769

Lee S, Seo PJ, Lee HJ, Park CM (2012) A NAC transcription factor NTL4 promotes reactive oxygen species production during drought-induced leaf senescence in *Arabidopsis*. Plant J 70: 831–844

Leivar P, Monte E (2014) PIFs: systems integrators in plant development. Plant Cell 26: 56–78

Leivar P, Quail PH (2011) PIFs: pivotal components in a cellular signaling hub. Trends Plant Sci 16: 19–28

Lesk C, Rowhani P, Ramankutty N (2016) Influence of extreme weather disasters on global crop production. Nature 529: 84–87

Li B, Chen L, Sun W, Wu D, Wang M, Yu Y, Chen G, Yang W, Lin Z, Zhang X, et al. (2020) Phenomics-based GWAS analysis reveals the genetic architecture for drought resistance in cotton. Plant Biotechnol J 18: 2533–2544

Li H, Handsaker B, Wysoker A, Fennell T, Ruan J, Homer N, Marth G, Abecasis G, Durbin R, et al. (2009) The sequence alignment/map format and SAMtools. Bioinformatics 25: 2078–2079

Liang Y, Liu HJ, Yan J, Tian F (2021) Natural variation in crops: realized understanding, continuing promise. Annu Rev Plant Biol 72: 357–385

Lipka AE, Tian F, Wang Q, Peiffer J, Li M, Bradbury PJ, Gore MA, Buckler ES, Zhang Z (2012) GAPIT: genome association and prediction integrated tool. Bioinformatics 28: 2397–2399

Liu J, Yao Y, Xin M, Peng H, Ni Z, Sun Q (2022) Shaping polyploid wheat for success: origins, domestication, and the genetic improvement of agronomic traits. J Integr Plant Biol 64: 536–563

Liu S, Li C, Wang H, Wang S, Yang S, Liu X, Yan J, Li B, Beatty M, Zastrow-Hayes G, et al. (2020) Mapping regulatory variants controlling gene expression in drought response and tolerance in maize. Genome Biol 21: 163

Liu S, Wang X, Wang H, Xin H, Yang X, Yan J, Li J, Tran LS, Shinozaki K, Yamaguchi-Shinozaki K, et al. (2013) Genome-wide analysis of *ZmDREB* genes and their association with natural variation in drought tolerance at seedling stage of *Zea mays* L. PLoS Genet 9: e1003790

Livak KJ, Schmittgen TD (2001) Analysis of relative gene expression data using real-time quantitative PCR and the $2^{-\Delta\Delta CT}$ method. Methods 25: 402–408

Lobell DB, Roberts MJ, Schlenker W, Braun N, Little BB, Rejesus RM, Hammer GL (2014) Greater sensitivity to drought accompanies maize yield increase in the U.S. Midwest. Science 344: 516–519

Machanick P, Bailey TL (2011) MEME-ChIP: motif analysis of large DNA datasets. Bioinformatics 27: 1696–1697

Mao H, Li S, Chen B, Jian C, Mei F, Zhang Y, Li F, Chen N, Li T, Du L, et al. (2022) Variation in *cis*-regulation of a NAC transcription factor contributes to drought tolerance in wheat. Mol Plant 15: 276–292

Mao H, Li S, Wang Z, Cheng X, Mei F, Chen N, Kang Z (2020) Regulatory changes in *TaSNAC8-6A* are associated with drought tolerance in wheat seedlings. Plant Biotechnol J 18: 1078–1092

Mao H, Wang H, Liu S, Li Z, Yang X, Yan J, Li J, Tran LS, Qin F (2015) A transposable element in a *NAC* gene is associated with drought tolerance in maize seedlings. Nat Commun 6: 8326

McKenna A, Hanna M, Banks E, Sivachenko A, Cibulskis K, Kernytsky A, Garimella K, Altshuler D, Gabriel S, Daly M, et al. (2010) The Genome Analysis Toolkit: a MapReduce framework for analyzing next-generation DNA sequencing data. Genome Res 20: 1297–1303

Morran S, Eini O, Pyvovarenko T, Parent B, Singh R, Ismagul A, Eliby S, Shirley N, Langridge P, Lopato S (2011) Improvement of stress tolerance of wheat and barley by modulation of expression of DREB/CBF factors. Plant Biotechnol J 9: 230–249

Nakai Y, Nakahira Y, Sumida H, Takebayashi K, Nagasawa Y, Yamasaki K, Akiyama M, Ohme-Takagi M, Fujiwara S, Shiina T, et al. (2013) Vascular plant one-zinc-finger protein 1/2 transcription factors regulate abiotic and biotic stress responses in *Arabidopsis*. Plant J 73: 761–775

Nakashima K, Ito Y, Yamaguchi-Shinozaki K (2009) Transcriptional regulatory networks in response to abiotic stresses in *Arabidopsis* and grasses. Plant Physiol 149: 88–95

O'Malley RC, Huang SC, Song L, Lewsey MG, Bartlett A, Nery JR, Galli M, Gallavotti A, Ecker JR (2016) Cistrome and epicistrome features shape the regulatory DNA landscape. Cell 165: 1280–1292

Pertea M, Kim D, Pertea GM, Leek JT, Salzberg SL (2016) Transcript-level expression analysis of RNA-seq experiments with HISAT, StringTie and Ballgown. Nat Protoc 11: 1650–1667

Qiu JR, Xiang XY, Wang JT, Xu WX, Chen J, Xiao Y, Jiang CZ, Huang Z (2020) MfPIF1 of resurrection plant *Myrothamnus flabellifolia* plays a positive regulatory role in responding to drought and salinity stresses in *Arabidopsis*. Int J Mol Sci 21: 3011

Scheet P, Stephens M (2006) A fast and flexible statistical model for large-scale population genotype data: applications to inferring missing genotypes and haplotypic phase. Am J Hum Genet 78: 629–644

Shavrukov Y, Baho M, Lopato S, Langridge P (2016) The TaDREB3 transgene transferred by conventional crossings to different genetic backgrounds of bread wheat improves drought tolerance. Plant Biotechnol J 14: 313–322

Shitsukawa N, Tahira C, Kassai K, Hirabayashi C, Shimizu T, Takumi S, Mochida K, Kawaura K, Ogihara Y, Murai K (2007) Genetic and epigenetic alteration among three homoeologous genes of a class E MADS box gene in hexaploid wheat. Plant Cell 19: 1723–1737

Tardieu F, Simonneau T, Muller B (2018) The physiological basis of drought tolerance in crop plants: a scenario-dependent probabilistic approach. Annu Rev Plant Biol 69: 733–759

Tester M, Langridge P (2010) Breeding technologies to increase crop production in a changing world. Science 327: 818–822.

Todaka D, Nakashima K, Maruyama K, Kidokoro S, Osakabe Y, Ito Y, Matsukura S, Fujita Y, Yoshiwara K, Ohme-Takagi M, et al. (2012) Rice phytochrome-interacting factor-like protein OsPIL1 functions as a key regulator of internode elongation and induces a morphological response to drought stress. Proc Natl Acad Sci USA 109: 15947–15952

Trapnell C, Roberts A, Goff L, Pertea G, Kim D, Kelley DR, Pimentel H, Salzberg SL, Rinn JL, Pachter L (2012) Differential gene and transcript expression analysis of RNA-seq experiments with TopHat and Cufflinks. Nat Protoc 7: 562–578

Van de Peer Y, Mizrachi E, Marchal K (2017) The evolutionary significance of polyploidy. Nat Rev Genet 18: 411–424

Wang X, Wang H, Liu S, Ferjani A, Li J, Yan J, Yang X, Qin F (2016) Genetic variation in ZmVPP1 contributes to drought tolerance in maize seedlings. Nat Genet 48: 1233–1241

Wu J, Yu R, Wang H, Zhou C, Huang S, Jiao H, Yu S, Nie X, Wang Q, Liu S, et al. (2021) A large-scale genomic association analysis identifies the candidate causal genes conferring stripe rust resistance under multiple field environments. Plant Biotechnol J 19: 177–191

Wu X, Feng H, Wu D, Yan S, Zhang P, Wang W, Zhang J, Ye J, Dai G, Fan Y, et al. (2021) Using high-throughput multiple optical phenotyping to decipher the genetic architecture of maize drought tolerance. Genome Biol 22: 185

Wu Y, Deng Z, Lai J, Zhang Y, Yang C, Yin B, Zhao Q, Zhang L, Li Y, Yang C, et al. (2009) Dual function of *Arabidopsis* ATAF1 in abiotic and biotic stress responses. Cell Res 19: 1279–1290

Xiang Y, Sun X, Gao S, Qin F, Dai M (2017) Deletion of an endoplasmic reticulum stress response element in a ZmPP2C-A gene facilitates drought tolerance of maize seedlings. Mol Plant 10: 456–469

Xiong H, Yu J, Miao J, Li J, Zhang H, Wang X, Liu P, Zhao Y, Jiang C, Yin Z, et al. (2018) Natural variation in OsLG3 increases drought tolerance in rice by inducing ROS scavenging. Plant Physiol 178: 451–467

Xu D, Deng XW (2020) CBF-phyB-PIF module links light and low temperature signaling. Trends Plant Sci 25: 952–954

Yamaguchi-Shinozaki K, Shinozaki K (2006) Transcriptional regulatory networks in cellular responses and tolerance to dehydration and cold stresses. Annu Rev Plant Biol 57: 781–803

Yang Y, Al-Baidhani HHJ, Harris J, Riboni M, Li Y, Mazonka I, Bazanova N, Chirkova L, Sarfraz Hussain S, Hrmova M, et al. (2020) DREB/CBF expression in wheat and barley using the stress-inducible promoters of HD-Zip I genes: impact on plant development, stress tolerance and yield. Plant Biotechnol J 18: 829–844

Yoo SD, Cho YH, Sheen J (2007) *Arabidopsis* mesophyll protoplasts: a versatile cell system for transient gene expression analysis. Nat Protoc 2: 1565–1572

Young MD, Wakefield MJ, Smyth GK, Oshlack A (2010) Gene ontology analysis for RNA-seq: accounting for selection bias. Genome Biol 11: R14

Yu S, Wu J, Wang M, Shi W, Xia G, Jia J, Kang Z, Han D (2020) Haplotype variations in QTL for salt tolerance in Chinese wheat accessions identified by marker-based and pedigree-based kinship analyses. Crop J 8: 1011–1024

Zhang H, Zhu J, Gong Z, Zhu JK (2021) Abiotic stress responses in plants. Nat Rev Genet 23: 104–119

Zhang L, Su W, Tao R, Zhang W, Chen J, Wu P, Yan C, Jia Y, Larkin RM, Lavelle D, et al. (2017) RNA sequencing provides insights into the evolution of lettuce and the regulation of flavonoid biosynthesis. Nat Commun 8: 2264

Zhang X, Mi Y, Mao H, Liu S, Chen L, Qin F (2020) Genetic variation in ZmTIP1 contributes to root hair elongation and drought tolerance in maize. Plant Biotechnol J 18: 1271–1283

Zhou Y, Chen M, Guo J, Wang Y, Min D, Jiang Q, Ji H, Huang C, Wei W, Xu H, et al. (2020) Overexpression of soybean DREB1 enhances drought stress tolerance of transgenic wheat in the field. J Exp Bot 71: 1842–1857

Zhu JK (2016) Abiotic stress signaling and responses in plants. Cell 167: 313–324